

EFFECT OF SHADOW IN BUILDING DETECTION AND BUILDING
BOUNDARY EXTRACTION

A THESIS SUBMITTED TO
THE GRADUATE SCHOOL OF NATURAL AND APPLIED SCIENCES
OF
MIDDLE EAST TECHNICAL UNIVERSITY

BY

ABDURRAHMAN YALÇIN

IN PARTIAL FULFILLMENT OF THE REQUIREMENTS
FOR
THE DEGREE OF MASTER OF SCIENCE
IN
ELECTRICAL AND ELECTRONICS ENGINEERING

DECEMBER 2008

Approval of the thesis:

**EFFECT OF SHADOW IN BUILDING DETECTION AND
BUILDING BOUNDARY EXTRACTION**

submitted by **ABDURRAHMAN YALÇIN** in partial fulfillment of the requirements for the degree of **Master of Science in Electrical and Electronics Engineering Department, Middle East Technical University** by,

Prof. Dr. Canan Özgen _____
Dean, Graduate School of **Natural and Applied Sciences**

Prof. Dr. İsmet Erkmek _____
Head of Department, **Electrical and Electronics Engineering Dept., METU**

Assist. Prof. Dr. İlkay Ulusoy _____
Supervisor, **Electrical and Electronics Engineering Dept., METU**

Prof. Dr. Uğur Halıcı _____
Co-Supervisor, **Electrical and Electronics Engineering Dept., METU**

Examining Committee Members:

Prof. Dr. Uğur Halıcı _____
Electrical and Electronics Engineering Dept., METU

Assoc. Prof. Dr. Tolga Çiloğlu _____
Electrical and Electronics Engineering Dept., METU

Assoc. Prof. Dr. Şebnem Düzgün _____
Geodetic and Geographic Information Technologies Dept., METU

Assist. Prof. Dr. İlkay Ulusoy _____
Electrical and Electronics Engineering Dept., METU

Assist. Prof. Dr. Alptekin Temizel _____
Informatics Institute, METU

Date: 04.12.2008

I hereby declare that all information in this document has been obtained and presented in accordance with academic rules and ethical conduct. I also declare that, as required by these rules and conduct, I have fully cited and referenced all material and results that are not original to this work.

Name, Last name: Abdurrahman Yalçın

Signature:

ABSTRACT

EFFECT OF SHADOW IN BUILDING DETECTION AND BUILDING BOUNDARY EXTRACTION

Yalçın, Abdurrahman

M.Sc., Department of Electrical and Electronics Engineering

Supervisor: Assist. Prof. Dr. İlkey Ulusoy

Co-Supervisor: Prof. Dr. Uğur Halıcı

December 2008, 90 pages

Rectangular-shaped building detection from high resolution aerial/satellite images is proposed for two different methods. Shadow information plays main role in both of these algorithms. One of the algorithms is based on Hough transformation, the other one is based on mean shift segmentation algorithm. Satellite/aerial images are firstly converted to YIQ color space to be used in shadow segmentation. Hue and intensity values are used in computing the ratio image which is used to segment shadowed regions. For shadow segmentation Otsu's method is used on the histogram of the ratio image. The segmented shadow image is used as the input for both of two building detection algorithms. In the proposed methods, shadowed regions are believed to be the building shadows. So, non-shadowed regions such as roads, cars, trees etc. are discarded before processing the image. In Hough transform based building detection algorithm, shadowed regions are firstly segmented one by one and filtered for noise removal and edge sharpening. Then, the edges in the filtered image are detected by using Canny edge detection algorithm. Then, line segments are extracted. Finally, the extracted line segments are used to construct rectangular-shaped buildings. In mean shift based building

detection algorithm, image is firstly segmented by using mean shift segmentation algorithm. By using shadow image and segmented image, building rooftops are investigated in shadow boundaries. The results are compared for both of the algorithms. In the last step a shadow removal algorithm is implemented to observe the effects of shadow regions in both of two implemented building detection algorithms. Both of these algorithms are applied to shadow removed image and results are compared.

Keywords: Building Detection, Hough Transform, Shadow Detection, Shadow Compensation, Satellite Images

ÖZ

BİNA BELİRLEME VE BİNA SINIRLARINI ÇIKARMADA GÖLGENİN ETKİSİ

Yalçın, Abdurrahman

Yüksek lisans, Elektrik Elektronik Mühendisliği Bölümü

Tez Yöneticisi: Yard. Doç. Dr. İlkyay Ulusoy

Ortak Tez Yöneticisi: Prof. Dr. Uğur Halıcı

Aralık 2008, 90 sayfa

Yüksek çözünürlüklü hava/uydu görüntülerinden dikdörtgen yapılı binaların bulunması iki farklı yöntem için önerilmektedir. Gölge bilgisi her iki algoritmada ana rolü üstlenmektedir. Algoritmalarından birisi Hough dönüşümü üzerine diğeri ise mean shift algoritması üzerine kurulmuştur. Uydu/hava görüntüleri gölge bölümlenmesinde kullanılmak için öncelikle YIQ renk uzayına çevrilmektedir. Renk ve yoğunluk değerleri gölge bölgelerini bölümlenme için kullanılan orantı resmini hesaplamak için kullanılmaktadır. Gölge bölümlenmesi için Otsu yöntemi orantı resminin histogramı üzerinde kullanılmıştır. Bölümlenmiş gölge resmi her iki bina belirleme algoritması için girdi olarak kullanılmaktadır. Önerilen metod da, gölge bölgelerin bina gölgeleri olduğu varsayılmaktadır. Böylece gölge olmayan bölgeler yollar, arabalar ve ağaçlar vb. resmi işlemeden önce ayrılmaktadır. Hough dönüşümü merkezli bina bulma algoritmasında öncelikle gölge bölgeler birer birer bölümlenmekte ve gürültü kaldırma ve kenar keskinleştirme için filtrelenmektedir. Daha sonra filtrelenmiş resimdeki kenarlar Canny kenar bulma algoritması ile belirlenmektedir. Daha sonra doğru parçaları çıkartılmaktadır. Son olarak çıkartılmış doğru parçaları dikdörtgen yapıdaki binaları oluşturmak için

kullanılmaktadır. Mean shift merkezli bina bulma algoritmasında ise öncelikle resim mean shift algoritması ile bölütlere ayrılmaktadır. Gölge bilgisi ve bölütlenmiş resim kullanılarak gölge sınırlarında bina çatıları araştırılmaktadır. Sonuçlar her iki algoritma için karşılaştırılmaktadır. Son olarak, her iki bina bulma algoritmasında gölge bölgelerinin etkisini gözlemlemek için bir gölge kaldırma algoritması uygulanmış ve birkaç resim üzerinde denenmiştir. Her iki algoritmada gölge kaldırılmış resme uygulanmış ve sonuçlar karşılaştırılmıştır.

Anahtar Kelimeler: Bina Belirleme, Hough Dönüşümü, Gölge Belirleme, Gölge Kaldırma, Uydu Görüntüleri

To My Family

ACKNOWLEDGMENTS

I express my deepest gratitude to my supervisor Assist. Prof. Dr. İlkey ULUSOY for her guidance and support throughout this study.

I also thank to Assoc. Prof. Dr. Şebnem DÜZGÜN for providing sample images used in this thesis and Örsan Aytekin for his valuable contributions.

I would like to thank my colleagues in ASELSAN Inc, Satellite Communications Systems Engineering Department for their advices, encouragements and insights throughout this research.

Also I would like to thank Ferhat KORKMAZ for being a good friend and supporter of mine and my family for their love, encouragement and full support.

TABLE OF CONTENTS

ABSTRACT	IV
ÖZ	VI
TABLE OF CONTENTS	X
LIST OF FIGURES.....	XII
LIST OF TABLES	XIV
1 INTRODUCTION.....	1
1.1 MOTIVATION	1
1.2 USED METHODOLOGY	2
1.3 THESIS OVERVIEW	4
2 BUILDING DETECTION FROM SATELLITE/AERIAL IMAGES.....	5
2.1 INTRODUCTION.....	5
2.2 EDGE DETECTION	7
2.3 HOUGH TRANSFORM	10
2.4 MEAN SHIFT SEGMENTATION	13
2.5 SHADOW	16
2.5.1 COLOR MODELS	18
3 PROPOSED BUILDING DETECTION METHOD.....	19
3.1 SYSTEM CHARACTERIZATION AND ARCHITECTURE	19
3.2 SHADOW DETECTION AND REMOVAL	21
3.3 HOUGH TRANSFORM AND BUILDING DETECTION	30
3.4 MEAN SHIFT BASED BUILDING DETECTION	40
4 IMPLEMENTATION AND RESULTS	44
4.1 INTRODUCTION.....	44

4.2	PERFORMANCE ANALYSIS.....	45
4.3	PARAMETER SELECTION	45
4.4	TEST RESULTS	51
4.5	EVALUATION OF THE RESULTS	73
5	DISCUSSION AND CONCLUSION.....	79
5.1	SUMMARY	79
5.2	DISCUSSION	79
5.3	FUTURE WORK	82
	REFERENCES.....	84

LIST OF FIGURES

FIGURES

FIGURE 1 COMPARISON OF THE EDGE DETECTOR PERFORMANCES.....	8
FIGURE 2 EDGE DETECTOR OUTPUTS.....	10
FIGURE 3 PARAMETRIC DESCRIPTION OF A STRAIGHT LINE	11
FIGURE 4 IMPLEMENTATION FLOWCHART OF SHADOW DETECTION AND REMOVAL ALGORITHM.....	21
FIGURE 5 RGB IMAGE.....	22
FIGURE 6 RATIO IMAGE.....	23
FIGURE 7 HISTOGRAM OF THE RATIO IMAGE.....	24
FIGURE 8 SHADOW REGIONS	25
FIGURE 9 CLEANED SHADOWED REGIONS	26
FIGURE 10 SHADOW BUFFER ZONE	27
FIGURE 11 SHADOW REMOVED IMAGE.....	28
FIGURE 12 SELECTED REGION	30
FIGURE 13 GRAY IMAGE OF THE SELECTED REGION	31
FIGURE 14 CANNY EDGE DETECTOR OUTPUT	31
FIGURE 15 EXTRACTED LINES	33
FIGURE 16 LINE-LINE INTERSECTION	34
FIGURE 17 GROUPED LINES	36
FIGURE 18 LINE GENERATION EXAMPLE.....	37
FIGURE 19 DETECTED BUILDINGS	37
FIGURE 20 BASIC LINE EXTRACTION AND BUILDING DETECTION FLOWCHART	39
FIGURE 21 MEAN SHIFT RESULT	40
FIGURE 22 DETECTED BUILDINGS	42
FIGURE 23 BUILDING BORDERS.....	42
FIGURE 24 EFFECT OF <i>START</i> AND <i>FINISH</i> PARAMETERS ON HOUGH TRANSFORM	47

FIGURE 25 EFFECT OF <i>THETA_RES</i> PARAMETER ON HOUGH TRANSFORM	48
FIGURE 26 EFFECT OF <i>PEAK_THR</i> PARAMETER ON HOUGH TRANSFORM	48
FIGURE 27 EFFECT OF <i>MINIMUMREGIONAREA</i> PARAMETER ON MEAN SHIFT ALGORITHM.....	49
FIGURE 28 EFFECT OF <i>SPATIALBANDWIDTH</i> PARAMETER ON MEAN SHIFT ALGORITHM	50
FIGURE 29 EFFECT OF <i>THR</i> PARAMETER ON MEAN SHIFT BASED BUILDING DETECTION ALGORITHM.....	50
FIGURE 30 TEST RESULTS #1	52
FIGURE 31 TEST RESULTS #1 CONTINUED	53
FIGURE 32 TEST RESULTS #2	54
FIGURE 33 TEST RESULTS #3	56
FIGURE 34 TEST RESULTS #4	58
FIGURE 35 TEST RESULTS #5	60
FIGURE 36 TEST RESULTS #6	62
FIGURE 37 TEST RESULTS #7	64
FIGURE 38 TEST RESULTS #7 CONTINUED	65
FIGURE 39 TEST RESULTS #8	66
FIGURE 40 TEST RESULTS #9	68
FIGURE 41 LOST L-SHAPE SHADOW REGIONS	73
FIGURE 42 FALSE POSITIVES DUE TO NON-UNIFORM SHADOW REGIONS AT THE OUTPUT OF THE MEAN SHIFT BASED BUILDING DETECTION ALGORITHM.....	74
FIGURE 43 EDGE IMAGE COMPARISON FOR TEST IMAGE #1	76
FIGURE 44 MEAN SHIFT BASED BUILDING DETECTION OUTPUTS	77

LIST OF TABLES

TABLES

TABLE 1 BUILDING DETECTION PARAMETERS	46
TABLE 2 IMAGE #1 RESULTS	53
TABLE 3 IMAGE #2 RESULTS	55
TABLE 4 IMAGE #3 RESULTS	57
TABLE 5 IMAGE #4 RESULTS	59
TABLE 6 IMAGE #5 RESULTS	61
TABLE 7 IMAGE #6 RESULTS	63
TABLE 8 IMAGE #7 RESULTS	65
TABLE 9 IMAGE #8 RESULTS	67
TABLE 10 IMAGE #9 RESULTS	69
TABLE 11 HOUGH TRANSFORM BASED BUILDING DETECTION ALGORITHM RESULTS .	69
TABLE 12 MEAN SHIFT BASED BUILDING DETECTION ALGORITHM RESULTS.....	70
TABLE 13 ALGORITHM PARAMETERS USED IN THE IMAGES	71
TABLE 14 RUN TIME EVALUATIONS.....	72
TABLE 15 AVERAGE BUILDING DETECTION RESULTS.....	72

CHAPTER 1

INTRODUCTION

1.1 MOTIVATION

Building detection in satellite/aerial images has been an active research field in aerial image understanding for many years. Some of building detection applications are urban mapping, land use analysis and also earthquake damage analysis. Building recognition methods are basically divided into two main categories which are edge-based and region based methods [1].

The edge-based methods use edge images in the initial stage. Edges are extracted by using well-known edge detectors e.g. Canny, Sobel etc. Original image is processed to extract edges in order to detect lines in the image. In the line detection part spurious edges are discarded and the remaining edges are grouped to form rectangular building shapes [2], [3]. In region-based building detection methods, the source image is segmented into regions and these regions are used in the building detection phase [1], [4], [5].

Many factors influence the quality of the building detection results. The time of the satellite image taken and the scene type are the main factors. The time of the satellite image taken affects the scene illumination. According to the sun direction, building occlusion amount changes during the day and makes building detection difficult.

Scene type of the image determines the amount of buildings in the image. Urban areas contain many buildings aligned very closely whereas suburban or rural areas contain only a few separated buildings. Also, roads, different types of buildings and roofs affect the building detection results in these areas. Although

roads are rarely occur in suburban areas, trees and vegetation make building detection difficult. Building shapes also affect detection algorithms. In the literature, different methods used for detection of different types of buildings such as rectangular, elliptical and circular shaped buildings.

Among the other factors, shadows are primarily concerned on this thesis. Although shadow regions can be used as an evidence of the desired object presence, in some conditions shadows result some difficulties in building detection methods. In edge based building detection methods, shadow boundaries cause strong gradient changes around building boundaries. These gradient changes can be easily detected by an edge detector and these shadow edges can be misclassified as building boundaries. Also in region based building detection methods, these shadow regions can be detected together with the true building boundaries.

The above mentioned problems make building detection a difficult problem in the digital image processing area.

The objective of this thesis is to develop a robust, reliable automatic rectangular shaped building detection system by using shadow information and to investigate effect of shadows on edge and region based building detection methods.

1.2 USED METHODOLOGY

The building detection methods proposed in this study use shadow information to make a decision on rectangular shaped buildings existence. Satellite/aerial images cover significant number of areas and include different types of structures in the images. These structures include trees, roads, airports, lakes, coastlines, seas and any type of land covers. The aim of the study is to eliminate these structures and to focus on buildings. To achieve this purpose, buildings are assumed to have shadows and only these regions are selected for building detection by the implemented algorithms. Although shadow geometry can be changed according to the building height, sun direction and the time of the image taken, it is assumed that rectangular shaped buildings have L-shaped shadow regions. So, implemented algorithms focused only these areas and this selection reduced false positives. Traditional methods in the literature apply implemented algorithms on the

whole image and select region of interests by using shadow information. In this study region selection is carried before the algorithm is applied and only these areas are processed. Also by selecting only shadow areas for detection, the computation time and false negatives are decreased.

Shadow segmentation is carried out using color ratios and thresholding techniques. The main reason for shadow segmentation is to eliminate vegetation and non-building structures such as roads, cars etc. Image data represented in RGB format is converted to YIQ format. The format conversion is required for ratioing color spaces to detect shadow regions. Y and Q components in YIQ image are divided to obtain ratio image to be used in segmentation. It has been observed that in the ratio image shadowed regions become easily detectable by using Otsu threshold. Also it is shown that an increase in the threshold eliminates misclassified regions.

Because of the implemented algorithm focuses on rectangular shaped building detection Hough transform is used for line detection. Hough based building detection algorithm uses shadow segmented image for selecting region of interests. The selected regions are processed by an edge detector to determine building borders. The most used edge detector algorithm in the literature, Canny edge detector algorithm, is chosen for edge detection step. The extracted edges are used to detect line segments from image by using Hough transform. The angle information of the detected lines is used for grouping connected lines. The missing parts of the building edges are added by using geometrical rules.

Mean shift based building detection algorithm uses mean shift segmented image and shadow information for detection. The algorithm first selects shadow regions and searches shadow boundaries for building rooftops in the opposite direction with respect to the given shadow direction.

Both algorithms are also applied to shadow removed images to investigate the effects of shadowed regions Shadow removal algorithm uses shadow boundary RGB values to recover shadowed regions. Mean and standard deviation values of the shadow regions and surroundings are calculated and used in the recovering process.

Nadir or near nadir view high resolution aerial images and satellite images are used in this thesis. The test images used in the thesis belong to the urban areas taken from Google Earth software with an altitude of 350m and IKONOS satellite images with 1m-pixel resolution.

1.3 THESIS OVERVIEW

The thesis chapters are organized as follows; Chapter 2 contains related literature survey.

In Chapter 3, shadow based automatic building detection system is explained in detail.

In Chapter 4, the implementation details are given for different test areas. Results obtained from aerial images are presented in this chapter.

Chapter 5 gives the summary, conclusion, and possible future work after this study.

CHAPTER 2

LITERATURE SURVEY:

BUILDING DETECTION FROM SATELLITE/AERIAL IMAGES

2.1 INTRODUCTION

Building detection from aerial images or satellite images is mainly used in urban mapping, land use analysis, environment monitoring and also in earthquake damage analysis. A significant amount of work has been performed in the field of aerial image understanding.

Krishnamachari and Chellappa [3], [6] used energy minimization method to detect building lines in aerial images. The used method is based on edge detection to extract lines in the images. Then, an energy function related with Markov Random Field is applied on the extracted lines to group exact building lines. The aim is to minimize the energy function to find building lines. But building lines are not always obtained due to poor quality of source images. So, snakes are used to complete the missing lines. A snake is a deformable contour which starts in an initial point in the image and advances to its final position by minimizing an energy function. Although snakes need a manually selected initial point to start convergence, researchers in [7] accomplished automatic selection of the initial point. In [8] a method is developed for automatic building detection. Two individual algorithms are implemented and used according to building types. One of the algorithms is based on Self Organizing Maps (SOMs). SOM's are used for training and creating segmented image. The second algorithm used edge detection method

for line extraction. Then, the extracted building lines are verified by using segmented image. In [2] multiple images are used to construct 3D description of the buildings. In the proposed method two images of the same scene taken at different times are used to extract building lines and construct 3D structure of the building. Building heights are verified by using wall and shadow information on the image. In the literature researchers also used different data sources besides aerial images. One of them is Digital Elevation Models (DEMs) [9], [10]. The main drawback of using DEMs is the low resolution of the data. But the availability of the height data makes them suitable for terrain modeling and 3D modeling of surface. Another data source is the topographic GIS data [11]. GIS data represents the real world with digital data based on raster or vector. Authors in [11] used GIS data for prior knowledge on the segmentation of the buildings. In the proposed approach fuzzy connectedness is used for segmentation. The seed point belonging to the object segmented is selected as the centroid of the GIS map building. Another approach based on fuzzy classification is described in [1]. The source data used in [1] are monocular grayscale aerial images. A different approach is presented by Levitt and Aghdasi in [12]. They used wavelet transform to extract building edges instead of using edge detectors. High frequency components yielded building edges in the images. To remove unwanted regions to be detected by wavelets, they performed low-pass filtering. Low-pass filter removed small regions such as cars and vegetation. Another approach is applied for high-rise buildings in monocular aerial images in [13]. They used vertical lines as the key evidence of the high-rise building extraction. Vertical lines are also used for the height extraction to be used in 3D modeling of the scene. Pesaresaj and Benediktsson in [14] proposed a method based on multiscale morphological segmentation. Their method performed better in complex image scenes. They also improved the main drawback of the multiscale method which requires heavily computational time. In [15] probabilistic method is used to extract buildings in high resolution panchromatic satellite images. The proposed method firstly segmented image into regions than used a probability function over regions to label selected regions as building. They also used shadow information, road distance etc. to verify the selected regions as buildings. The main

drawback of the method is the dependency of the shadow model to the building. An invariant shadow model will robust the proposed method. In [16], [17], [18] and [19] shadow and wall evidence is used for the verification of the extracted buildings which is common in the literature. Authors used monocular oblique aerial images to detect and describe buildings in 3D. Oblique views provided them more evidence for verification. They used shadow information to determine the height of the building. In [20], an approach was developed to update the buildings of existing vector database. They used image classification, Digital Elevation Models and object extraction techniques. Since there is no perceptual grouping used in the building extraction stage, some misleading results have occurred at the output. In [21] Digital Elevation Model and ortho image is used for building detection and 3D reconstruction. By using digital elevation model, every above-ground element is classified as rectangle elements. To eliminate false positives, Hausdorff measure is used. In [22] a three layer perceptron neural network is trained for detection of buildings in satellite images, but in the training phase an operator interaction is needed to select the training sets.

2.2 EDGE DETECTION

An edge is a boundary region in the image which has high gradient magnitude. Edge detection removes redundant information in the images and extracts boundaries of the interested regions. In the literature, edge detection methods are divided into two categories, Laplacian based and gradient based. The Laplacian based edge detector searches zero crossings in the second derivate of the image whereas gradient based edge detectors look maximum and minimum values in the first derivate of the image for edge detection [24]. In [23], the performance of 11 different edge detectors is analyzed. The results are given in Figure 1. Among the edge detection operators “Roberts, Sobel and Prewitt” can be shown as gradient based edge detectors and Laplacian of Gaussian can be shown as Laplacian based edge detectors.

Results for the Dataset of 50 Object Images										
	Heit	Iver	Cann	Bezde	Berg	Blac	Roth	Sobe	Smit	Sark
Heitger	*									
Iverson	46	*								
Canny	46	31	*							
Bezdek	49	29	24	*						
Bergholm	49	36	39	39	*					
Black	50	40	34	35	24	*				
Rothwell	50	45	49	48	49	40	*			
Sobel	50	47	49	49	48	44	45	*		
Smith	50	49	50	50	49	48	40	9	*	
Sarkar	50	48	50	47	48	43	39	9	30	*
Ahuja	45	38	33	34	32	31	22	10	16	12

Results for the Dataset of 10 Aerial Images

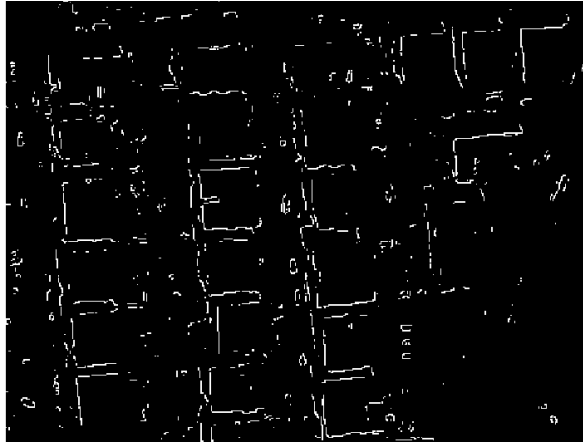
Figure 1 Comparison of the edge detector performances [23]

Note: Entries in the tables indicate the number of times that the column-named detector had better than the row-named detector.

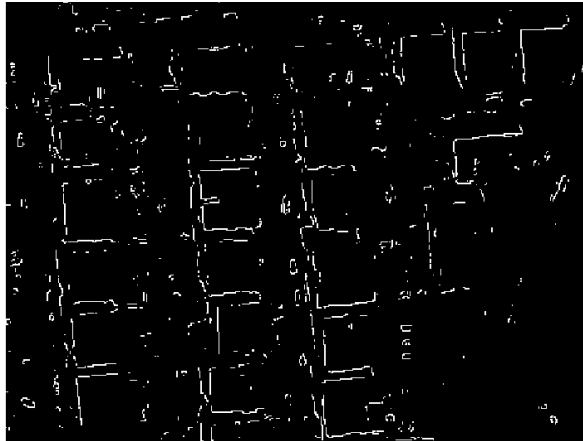
In this thesis, canny edge detector is chosen for edge detection. The edge detection results for different edge detectors are given in Figure 2.



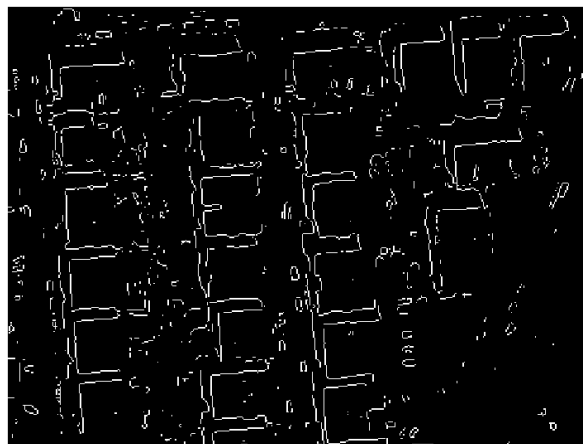
a) Original Image



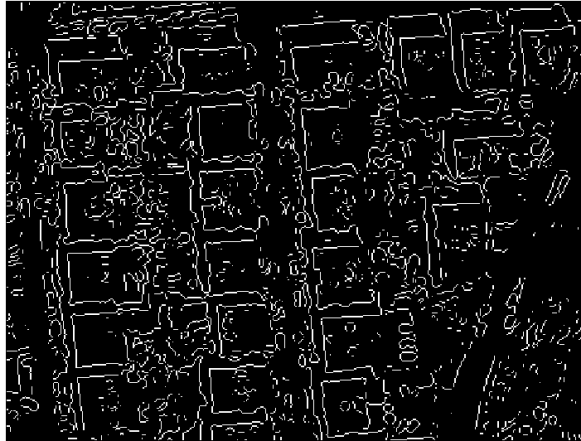
b) Roberts Edge Detector Output



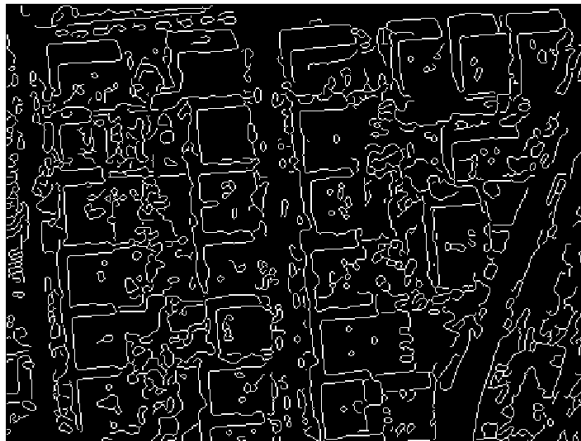
c) Sobel Edge Detector Output



d) Prewitt Edge Detector Output



e) LoG Edge Detector Output



f) Canny Edge Detector Output

Figure 2 Edge Detector Outputs

2.3 HOUGH TRANSFORM

The Hough transform is mainly used for detection of lines, circles, ellipses, etc. In this study Hough transform is used for line detection to create rectangles around buildings. The Hough transform took its general form by Richard Duda and Peter Hart in 1972, who called it a "generalized Hough transform"[25] after the related 1962 patent of Paul Hough [26]. Hough transform uses parametric equations

to detect lines, circles and other shapes. These equations are used on the edge images. These edge images can be obtained from different edge detectors. The main advantage of the Hough transform is that it is relatively unaffected by image noise.

In this study Hough transform is used to detect line segments. A line segment can be described as:

$$x \cos \theta + y \sin \theta = r \quad (2.1)$$

where r is the length of a normal from the origin to this line and θ is the angle between r and X-axis. Figure 3 shows the parametric description of a straight line. Normal and angle values (r, θ) are constant for every point (x, y) on this line.

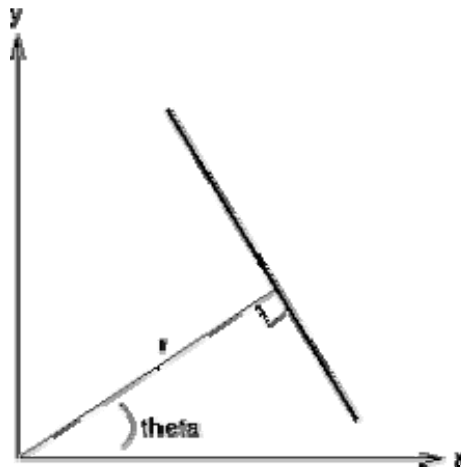


Figure 3 Parametric description of a straight line [27]

As explained before Hough transform uses edge points to extract line segments. Every edge point coordinates correspond x and y values in Eq 2.1. The algorithm simply searches for possible (r, θ) values. Each (r, θ) pairs correspond a curve (sinusoid) in Hough parameter space. Intersection point of this curves yield possible (r, θ) pairs we seek. But as we know, infinite number of lines can pass

through a single point, the algorithm uses accumulator arrays to store possible (r, θ) pairs. For every edge point, algorithm searches possible (r, θ) pairs and increment this pair in the accumulator array. When the algorithm finishes, peak values in the accumulator array represent line evidence in the image.

Detection of other shapes is out of the scope of this thesis. But following equation can be used to detect circles in images.

$$(x - a)^2 + (y - b)^2 = r^2 \quad (2.2)$$

where a and b are the coordinates of the center of the circle and r is the radius. In this case we have three coordinates so accumulator array size increased from 2D to 3D. It can be seen that when the parameters increase, algorithm complexity also increases polynomially. It also increases computation time which makes algorithm inefficient [27], [28].

Hough transform has been used widely in the literature with many different methods. In [29] Hough transform is used for feature extraction and the extracted invariant features are fed to a Neural Network to train and learn the shapes. The proposed study is used for higher level object recognition. Chatzis and Pitas [30] used fuzzy classification to detect parameters in Hough space. Ioannou and Dugan [31] used Hough transform for detection of polygonal shapes. In [32] a different approach is proposed to detect lines in the images. They applied Hough transform three times and called as Cascaded Hough Transform (CHT). CHT is used for detection of layered straight lines, vanishing points and vanishing lines. They applied Hough transform on the output of a previous Hough transform. The first Hough transform extract straight lines in the image, the second Hough transform maps first Hough output to a new (x, y) space and these points represent line intersections and the last Hough transform detects collinear line intersections. The disadvantage of the proposed method is the necessity of huge amount of memory.

In [34] the memory requirements in Generalized Hough Transform [35] are reduced by using higher level shape representation features. In [36] Barret and Petersen used Hough accumulator array for peak extraction. In the proposed method Hough transform is applied and accumulator array is formed. They searched

sinusoids on the Hough space and when the sinusoid has passed at least two peaks in the accumulator array these new points copied to another array that is directly related to the image. In [41], a windowed Hough transform method is proposed. In the proposed method Hough transform is applied only a small portion of the image which lies in the window and peaks are extracted. From these peaks rectangles are formed if they satisfy some geometrical conditions.

In [37] Kiryati and YIa-Jaaski used Hough transform for circular shape detection. Their method uses probabilistic approach and by using adaptive poll size the computation time is reduced. It has also investigated that Hough transform can also be used for triangle detection [33]. In [33] randomized Hough transform is used to directly detect triangles.

Hough transformation can be also used for ellipse shape detection. Since an ellipse is characterized by five parameters: center position coordinates; lengths of the major and minor axes; and the orientation of the major axis five dimensional accumulators are needed. By using basic Hough transform this computation will take too much time. There are some methods in the literature to reduce the computation time [38], [39].

In [40], another Hough transform method is applied in circular object recognition. They used geometrical relations to detect circular objects. The original image is firstly segmented into binary image and 4-connected pixels are labeled. Then, those regions with shape parameters satisfy certain conditions are recognized as circular objects.

2.4 MEAN SHIFT SEGMENTATION

Mean shift algorithm is a nonparametric clustering approach which is widely used in pattern recognition tasks. In [50] Mean shift algorithm is used for discontinuity preserving filtering and image segmentation. Mean shift procedure used in [50] is explained in this section.

Given n data points $x_i, i = 1, 2, \dots, n$ in the d -dimensional space R^d , the kernel density estimator with kernel $K(x)$ and bandwidth h is given in Eq. (2.3).

$$f(x) = \frac{1}{nh^d} \sum_{i=1}^n K\left(\frac{x-x_i}{h}\right) \quad (2.3)$$

In [50], radially symmetric kernels are preferred which is given in Eq. (2.4)

$$K(x) = c_{k,d} k\left(\|x\|^2\right) \quad (2.4)$$

where $k(x)$ is the profile of the kernel and $c_{k,d}$ is the normalization constant.

If we replace $k(x)$ in Eq (2.3) with Eq (2.4) equation becomes;

$$f(x) = \frac{c_{k,d}}{nh^d} \sum_{i=1}^n k\left(\left\|\frac{x-x_i}{h}\right\|^2\right) \quad (2.5)$$

In the proposed method the first step is to find the modes of the density function without estimating the density. This is achieved by finding zeros in the gradient of the density. From the gradient of the density estimator, mean shift vector is obtained. The details of the process are explained in [50]. The mean shift vector always points in the direction of maximum increase in the density. As the algorithm runs for the selected kernel (window), density estimator is calculated first and by using density estimator, means are calculated by using Eq (2.6).

$$y_{j+1} = \frac{\sum_{i=1}^n x_i g\left(\left\|\frac{y_j - x_i}{h}\right\|^2\right)}{\sum_{i=1}^n g\left(\left\|\frac{y_j - x_i}{h}\right\|^2\right)} \quad j = 1, 2, \dots \text{ and } g(x) = -k'(x) \quad (2.6)$$

From the calculated means, mean shift vector is obtained by using Eq.(2.7).

$$m_{h,G}(y_j) = y_{j+1} - y_j \quad (2.7)$$

Algorithm stops when Eq.(2.7) equals to zero i.e current mean and next mean values are equal.

Before processing image, the algorithm needs RGB images to be converted to another color spaces such as $L^*u^*v^*$ or $L^*a^*b^*$ in which color differences correspond to Euclidean distances in the color space. An image can be simply

defined as 2D lattices (arrays). These arrays (pixels) contains p-dimensional vectors where $p = 1$ for grayscale images and $p = 3$ for colored images. Spatial domain of the image corresponds to the space of the lattice and gray level, color or spectral information is stored in the range domain. Because of these two domains, two kernels are used in [50].

$$K_{h_s, h_r}(x) = \frac{C}{h_s^2 h_r^p} k\left(\left\|\frac{x^s}{h_s}\right\|^2\right) k\left(\left\|\frac{x^r}{h_r}\right\|^2\right) \quad (2.8)$$

where x^s is the spatial part of the feature vector, x^r is the range part of the feature vector, $k(x)$ is the profile of the kernel, h_s and h_r are the kernel bandwidths and C is the normalization constant.

The implemented algorithm in [50] has four main steps given below;

1. For each pixel x_i , $i = 1, 2, \dots, n$ in the image, initialize $j=1$ and $y_{i,1} = x_i$. Then compute $y_{i,j+1}$ according to Eq. (2.6) until convergence, $y = y_{i,c}$. Then assign the value of convergence $y_{i,c}$ to the pixel x_i . This process is called as mean shift filtering.
2. Group clusters $(C_p)_{p=1,2,\dots,m}$ by using $y_{i,c}$ values which are closer than h_s in the spatial domain and h_r in the range domain.
3. For each cluster assign a label.
4. Discard spatial regions containing less than M pixels.

The implemented algorithm [50] needs h_s and h_r values and also the minimum region size (M) for segmentation. Minimum region size is required for clustering process. If a region size is smaller than the minimum region size, then this region is eliminated. By changing these parameters, algorithm results can be improved.

2.5 SHADOW

Shadow occurs when objects occlude the direct light projected from an illumination source. In the literature, two types of shadow are defined: cast shadow and self (attached) shadow. The first one occurs when an object shadow projects on another object, such as the ground. The second one is the shadow of the object itself which is not illuminated by light source [42].

In urban aerial images, shadows are usually caused by nearby objects when they are not illuminated by sun. By looking at shadow, one can determine the position of the light source and geometrical shape of the casting object. But objects in the shadows are hardly recognizable. As a result, cast shadows cause loss of feature information, false color tone, shape distortion of objects in the shadow area [43].

Shadows are detected by two different detection approaches in the literature. These methods are model based and property based methods. The model based methods use prior knowledge of the direction of the illumination source and the 3D geometry of the scene to calculate positions of shadows. Since illumination source direction is not always available; this method is rarely used. The property based shadow detection methods use hue, intensity and geometry structure of shadows for detection. This method is widely used. Generally, shadow areas are believed to have low intensity values than surrounding areas. For grayscale images, shadows can be detected by using an intensity threshold. But for color images, intensity thresholding techniques may misclassify some areas which have lower intensity values. Because of this reason other methods, such as RGB ratios and photometric color invariants based methods are proposed in the literature. In RGB ratio based methods, intensity values in all R, G and B bands decrease with same ratio in uniform casting surface after shadow. So, thresholding techniques can be applied to ratio images to detect shadows. In photometric color invariant based methods, thresholding results of un-shadowed regions are subtracted from original image to detect shadows [44].

There are several techniques in the literature in detecting shadows in black and white aerial images and colored images. In the literature serious work has been

done on shadow detection and compensation and shadow information is used for the verification of the building detection algorithms [15], [16], [17], [18], [19].

In [43], the proposed approach uses spectral ratioing and automatic thresholding techniques for shadow detection. The proposed method doesn't require a prior knowledge of the illumination source, shadow alignment or information on the scene. They used two-step histogram matching technique to compensate shadow regions and applied the algorithm on different color domains.

In [45] the proposed method detects changes of buildings by comparing shadows of the buildings which are taken at different times. They used a shading model based on a relation between sun illumination and 3-D shapes of buildings which occlude the incident light. Since 3-D representation of the scene takes too much computation time, they used 2-D images.

In [42] a hierarchical shadow detection algorithm for color aerial images is presented. The proposed method overcomes the drawbacks of different brightness and illumination conditions in different images and the complexity of aerial images. The proposed method used pixel level classification and region level verification to detect shadow areas.

In [46] the proposed method used image segmentation and edge detection methods for shadow detection. Image is segmented into same color regions and edge detection is performed. By using edge image, each edge regions are searched for illumination change.

In [47] the proposed method uses Bayesian assumption to shadow detection and removing. On the basis of the proposed method there are some user supplied inputs which are called as quad map (for ex: shadowed region, non-shadowed region etc.). According to the inputs some Bayesian equations are solved and shadows are removed from the image.

In [48] a histogram modification method is used for shadow removal. At first image is partitioned to I by I blocks and for each block the mean value is calculated. The extracted mean values are mapped to a new array. In the new array the median value is calculated. The mean values below the median value are

identified as shadowed region and a quantization coefficient is multiplied by every elements of the block in the original image.

In [49] probabilistic method is applied to segment image into shadow and non-shadowed regions. The probability function is implemented on low frequency component of the original image. By using posteriori probabilities, every shadow pixel intensity and saturation values are updated in the last stage.

2.5.1 COLOR MODELS

Depending on the method different color models are used in the literature. In this thesis YIQ color model is used and described in the following section.

2.5.1.1 YIQ COLOR MODEL

In YIQ color model, Y is proportional to the luminance value, which corresponds to intensity, and I and Q describe the chroma, which corresponds to hue and saturation values [43]. RGB images can be converted into YIQ images by using Eq. (2.9) [43].

$$\begin{bmatrix} Y \\ I \\ Q \end{bmatrix} = \begin{bmatrix} 0.299 & 0.587 & 0.114 \\ 0.596 & -0.275 & -0.321 \\ 0.212 & -0.523 & 0.311 \end{bmatrix} \begin{bmatrix} R \\ G \\ B \end{bmatrix} \quad (2.9)$$

CHAPTER 3

PROPOSED BUILDING DETECTION METHOD

3.1 SYSTEM CHARACTERIZATION AND ARCHITECTURE

In this chapter the architecture of the implemented building detection method is presented. The major goal of the proposed method is to detect buildings in the satellite images by using shadow information and investigate the effect of the shadows. The principal approach of the method is to classify shadowed regions as a candidate of building presence and apply implemented algorithms to find building boundaries. Basically, edge based and region based building detection methods are applied on the images. Building lines are extracted by using Hough transform and regions are extracted by using Mean shift segmentation algorithm. Shadow effect is investigated for both algorithms. For shadow detection and removal, the method proposed in [43] is implemented. Both algorithms are first applied to original images and then to shadow removed images. The results of both algorithms on original images and shadow removed images are analyzed.

The implemented algorithms are applied only to the shadowed areas not to the whole image. By selecting only shadow areas, computation time and also false negatives are decreased. The implemented algorithm in [43] is not computationally expensive and performed well for all RGB images. The implemented algorithm uses ratio images and thresholding techniques to find shadowed regions.

Mean shift segmentation algorithm in [50] is used for region based building detection method. The aerial images are segmented by using codes in [50] and results are examined to detect building regions. The algorithm is performed very

fast and effectively segmented images. In the last part, shadow information is used for verification.

The organization of the implementation steps will be as follows; Section 3.2 introduces how the image is segmented into shadowed areas and represents shadow removal algorithm. Section 3.3 covers Hough transform and line grouping technique. Section 3.4 describes the mean shift segmentation based building detection algorithm.

3.2 SHADOW DETECTION AND REMOVAL

The proposed method starts with the shadow detection process. For shadow detection and removal algorithm, the methods used in [43] are implemented. According to [43] the best results are achieved in the HIS and YIQ color domains. In this study YIQ color domain is used due to its simplicity to implement. Figure 4 shows the flowchart of the algorithm.

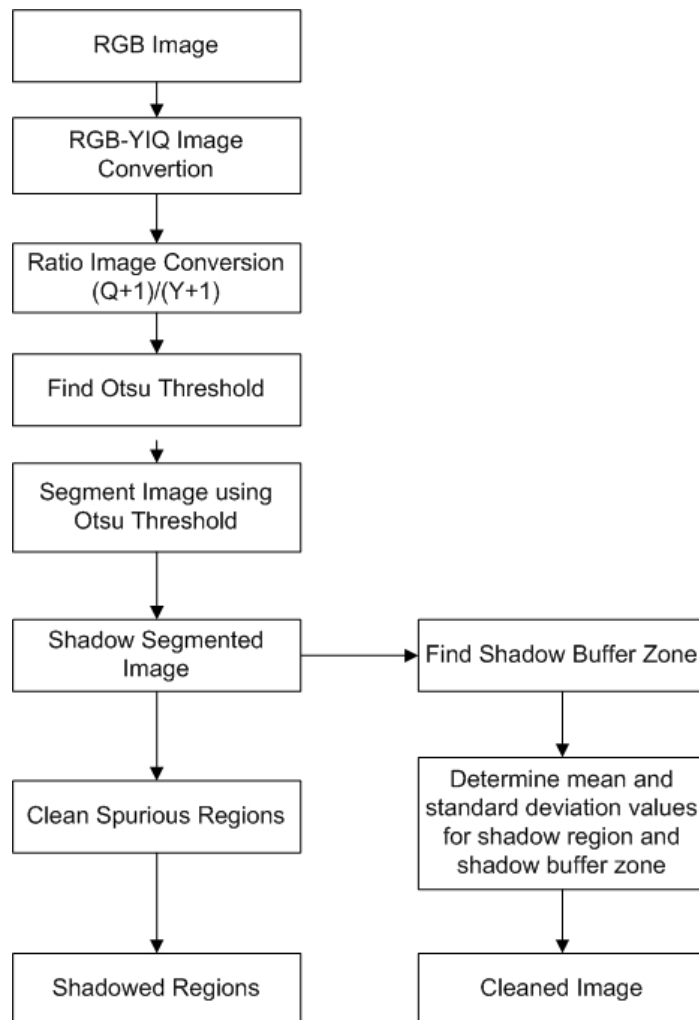


Figure 4 Implementation flowchart of shadow detection and removal algorithm

Figure 5 shows a sample RGB image which is used during the implementation.



Figure 5 RGB Image

In the first step, RGB satellite/aerial images are converted to YIQ color space. After RGB-YIQ conversion the method in [43] is applied for segmentation. From the hue and intensity values a ratio image is obtained. In YIQ image, hue and intensity values correspond to Q and Y components. Ratio image is obtained by using spectral ratioing techniques which is the division of hue component values to intensity component values. First hue and intensity values are incremented by 1 and then hue values are divided by the intensity values [43]. The ratio image formula in [43] is presented in Eq.3.1;

$$\text{ratio image} = \frac{Q+1}{Y+1} \quad (3.1)$$

The ratio image for Figure 5 is given in Figure 6. In the ratio image shadow regions have brighter color contents according to their surroundings. The ratio

image enhances the hue property of the shadows, so pixels in shadowed regions have higher values than pixels in non-shadowed regions in the ratio image [43].



Figure 6 Ratio Image

The ratio image is then segmented by using Otsu's method [52]. The Otsu method is applied to the histogram of the ratio image. The aim is to automatically determine the threshold for segmenting shadowed regions. The Otsu's method finds an optimal threshold k which maximizes [52];

$$P(k) = \frac{[\mu_T(\omega(k) - \mu(k))]^2}{\omega(k)[1 - \omega(k)]} \quad (3.2)$$

where;

$$\omega(k) = \sum_{i=1}^k p_i \quad (3.3)$$

$$\mu(k) = \sum_{i=1}^k ip_i \quad (3.4)$$

$$\mu_T = \mu(L) = \sum_{i=1}^L ip_i \quad (3.5)$$

where L is the gray levels, p_i is the probability of the pixels with grey level i in the image, $\mu(L)$ is the total mean level of the original image, $\omega(k)$ and $\mu(k)$ are the zero and first-order cumulative moments of the histogram up to the k th level. The algorithm details are given in [52]. In this study, Matlab built-in functions are used for Otsu threshold selection. Figure 7 shows histogram of the ratio image and selected threshold ($k=167$).

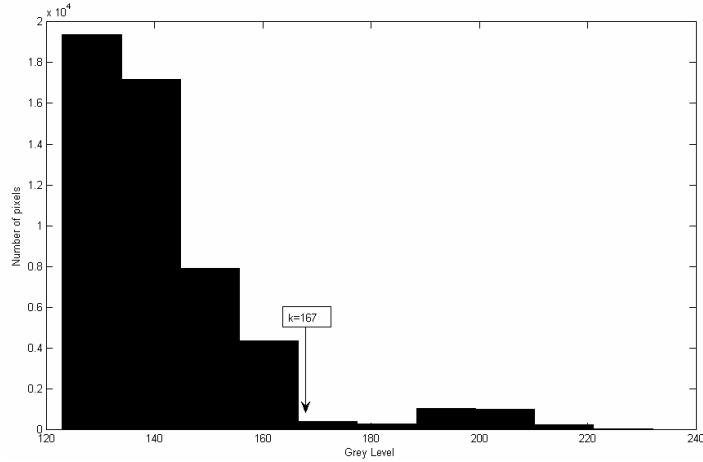
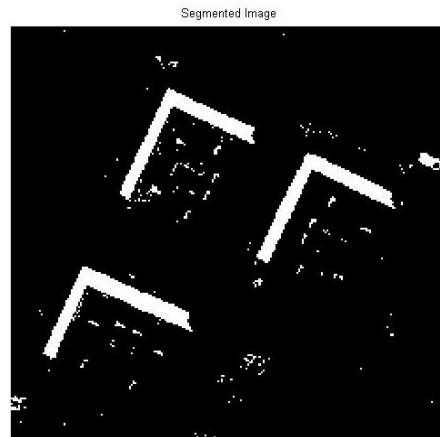


Figure 7 Histogram of the ratio image

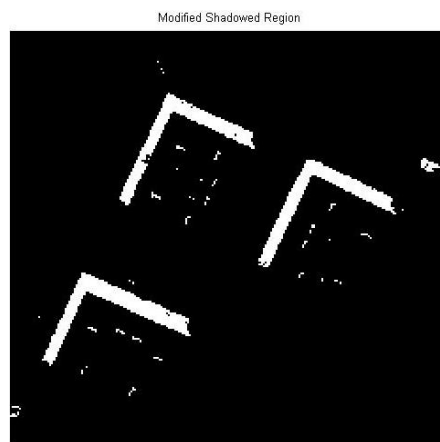
After selecting segmentation threshold, image is segmented into shadow regions. Shadow detection output is a binary image in which ratio image pixel values larger than the threshold are labeled with "1" others with "0". The segmented image is given in Figure 8.

Although Otsu threshold divides image histogram into two pieces sometimes there are some misclassified regions in the segmented image. For a calculated threshold, dark colored regions or objects may be misclassified. For this reason the

Otsu Threshold is increased in this study to reduce misclassified region areas. For the sample image Otsu threshold is increased by 10% of the original threshold. Figure 8 shows segmentation results with original and increased threshold value.



a)



b)

Figure 8 Shadow Regions a) Original threshold is used b) Increased threshold is used

Then, morphological operations are performed on the segmented image to remove small spurious regions. Holes in the images are filled and morphological

open and close operations are applied to the image respectively. While morphological opening breaks narrow strokes, morphological closing fuses short gaps between objects. The result is given in Figure 9.

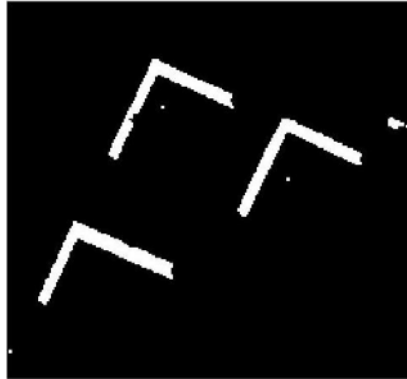


Figure 9 Cleaned Shadowed regions

The last step in the algorithm is shadow removal. Shadow removal algorithm tries to find mean values of the surroundings of the shadow regions and stores these values into shadowed regions. Mean values are extracted for all Red, Green and Blue color bands. Morphological operations are used to find shadow surroundings and these regions are called as shadow buffer zones [43]. Figure 10 shows buffer zone for the sample image.

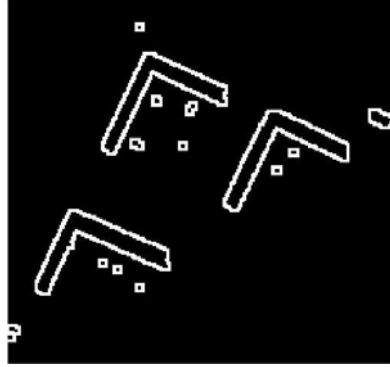


Figure 10 Shadow Buffer Zone

First of all, for each shadow region, the related buffer zone is extracted firstly. Instead of using morphologically cleaned image, the rough shadow regions are used for shadow buffer zone extraction. The reason that lies in this selection is the loss of data at shadow edges during morphological cleaning operation.

Then the pixels on the buffer zone are determined and these pixels' values in RGB image are extracted. Mean and standard deviation values are determined for Red, Green and Blue bands using these pixels' RGB values. At the same time, the mean and standard deviation values are also extracted for the selected shadow region. Then, the pixel values in the shadow regions are updated using Eq.3.6 [43] for all three bands. The shadow removed image is given in Figure 11.

$$D N_s ' = \frac{\sigma_n}{\sigma_s} D N_s + m_n - \frac{\sigma_n}{\sigma_s} m_s \quad (3.6)$$

where

DN_s : Brightness value of shadow area

DN_s' : adjusted value of DN_s

m_n : mean brightness of the shadow buffer zone (reference)

σ_n : std. deviation of brightness of the shadow buffer zone

m_s : mean brightness of shadow area

σ_s : std. deviation of brightness of shadow area

Enhanced Image



Figure 11 Shadow Removed Image

FLOWCHART OF THE SHADOW DETECTION AND REMOVAL ALGORITHM

The procedural flow chart of the method is represented below:

- i. RGB image is converted to YIQ image.
- ii. From YIQ image $\frac{(Q+1)}{(Y+1)}$ ratio image is obtained.
- iii. Otsu threshold is found from ratio image.
- iv. The Otsu threshold is used to segment the ratio image. Regions below the Otsu threshold are classified as shadowed regions and the other regions are classified as non-shadowed regions.
- v. Fill holes in the segmented image.
- vi. Remove small spurious regions from image by applying morphological open and close operations respectively.
- vii. Output cleaned image.
- viii. From the image in iv extract shadow buffer zone for the selected shadow region.
- ix. Determine buffer zone pixels and by using these pixels extract Red, Green and Blue values from original RGB image.
- x. Determine mean and standard deviation values for both shadow buffer zone and shadow region.
- xi. Update pixel values in shadow region by using formula given in Eq.3.6.
- xii. Output shadow removed image.

3.3 HOUGH TRANSFORM AND BUILDING DETECTION

The detected shadow region image is used as the input for both of the algorithms. The Hough based building detection algorithm extracts line segments and decides which one of the lines are the building lines.

At first, the algorithm chooses shadowed regions from the original image. In this study shadowed regions are assumed to have L-shape regions i.e. shadows are formed around the two sides of the buildings. This selection simplifies the verification.

The region selection criterion depends on L-shape shadow hypothesis and according to this hypothesis a rectangle region is selected which contains shadow borders. To increase building area in the image, the shadowed regions are selected 20 % larger than the original sizes. Increasing factor can be changed to any value. In this study it is chosen 20% of the original size. Too much increase in this value will add nearest objects to the shadowed area. Figure 12 shows original and modified region selection.

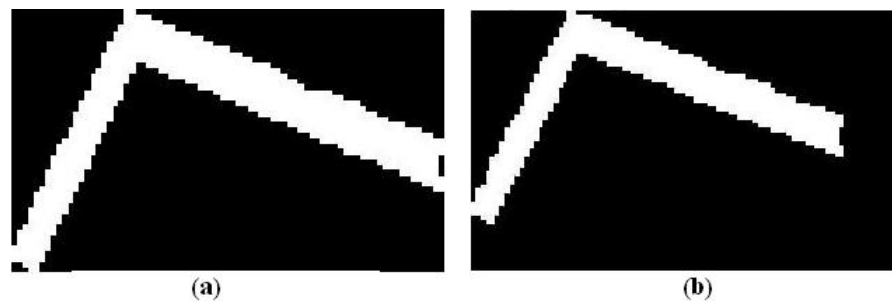


Figure 12 Selected Region a) Original region b) Increased region

Since Hough transform uses edge image for line extraction, the next step in the algorithm will be edge detection. But as seen on Figure 12 selected regions are

binary images. For further processing these regions should have pixel values rather than 0's and 1's. For this reason selected regions are extracted from gray level image. Figure 13 shows gray image of the selected region.



Figure 13 Gray image of the selected region

The selected gray image is then processed with Canny edge detector to extract edges for the line extraction stage. The minimum and maximum thresholds for the Canny edge detector are extracted automatically from the image. Figure 14 shows edge detector output.



Figure 14 Canny Edge Detector Output

After edge image is obtained, the output is used for line extraction. Line extraction step begins with Hough transform. For all white points (shadow) in the edge image Hough transform calculates (r,θ) pairs. In the proposed study for θ values a resolution value is defined between two θ values. *Theta_res* determines how θ values will be incremented. For the sample image this value is chosen “1”, so θ values incremented one by one. Theta resolution controls the amount of the detected line segments. Increasing this value decreases the number of detected lines and this will yield good results when too many lines are detected. If we decrease this value detected line numbers are increased and will yield unwanted lines to be created.

The Hough transform algorithm creates a matrix which is called Hough matrix. Hough matrix rows and columns are the (r,θ) values in the image. Initially each cell in the Hough matrix is set to zero. For every non-background point in the edge image r value is calculated for every θ value. Then calculated (r,θ) pair in the Hough matrix is incremented. The values in the Hough matrix cells correspond to how many pixels in the image have corresponding (r,θ) pairs.

After all pixels have been processed another threshold is used to select (r,θ) pairs. The selection criterion depends on Hough matrix contents. As it is explained before, the contents of the Hough matrix cells are the pixels which have corresponding (r,θ) pairs. So, larger values in the Hough matrix are the candidates for the selection. The maximum value of the Hough matrix is determined and multiplied with *Peak_Thr* parameter. So, if the Hough matrix values are bigger than *Peak_Thr x max (Hough Matrix)*, the (r,θ) pair is selected for further processing. For sample image *Peak_Thr* is chosen to be 0,7.

The next step is to create line segments in the image. The image is searched to find pixels which have selected (r,θ) values. These pixels are then used to generate line segments.

The first criterion in the line generation is to determine minimum line length. The pixels which have same (r, θ) values are grouped together to generate line segments according to minimum line length criterion. If generated line segment length is smaller than the minimum line length than these line segments are

excluded. For the sample *min_length* is chosen to be 2 pixels. Increasing this threshold removes some unwanted lines but due to the edge detector output it can also miss desired lines.

The second criterion is to merge small line segments into larger line segments. If the distance between two line segments is smaller than a threshold value, these line segments are merged to generate a larger line segment. For the sample image *fill_gap* threshold is chosen to be 10 pixels. If the distance between two line segments is larger than 10 pixels then they are not grouped.

The line extraction results are given in Figure 15. For three shadow regions, beginning of the lines are marked with yellow and ends with red.



Figure 15 Extracted lines for a) Building #1 b) Building #2 c) Building #3

After all lines are extracted, geometrical rules are applied to generate rectangles. In this study two rules are used for line selection.

According to the first rule, algorithm selects lines one by one and calculates angles between other lines. Because of the image resolution and edge detector output building lines do not always have ninety degree corners. So, in the algorithm not only ninety degree is searched but also ± 5 degrees around ninety are searched.

This value is set by *start* and *finish* parameters. If the angle between selected line and other line is between *start* and *finish* then these lines are grouped together.

The second rule eliminates some of these grouped lines. If the distances of starting or ending points of the grouped lines are above *dist_thr* then these lines are removed.

After verifying line grouping rules the next step in the algorithm is to intersect these grouped lines. It is observed that some of the grouped lines do not intersect each other and small distances occur between them. So, these lines have to be merged before generating rectangles around buildings. The intersection of two lines L_1 and L_2 , where L_1 has points (x_1, y_1) and (x_2, y_2) , and L_2 has points (x_3, y_3) and (x_4, y_4) , is given in Figure 16.

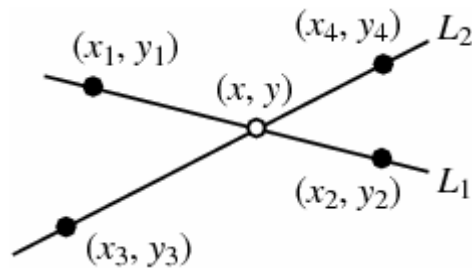


Figure 16 Line-Line Intersection [51]

$$x = \frac{\begin{vmatrix} x_1 & y_1 & x_1 & 1 \\ x_2 & y_2 & x_2 & 1 \\ x_3 & y_3 & x_3 & 1 \\ x_4 & y_4 & x_4 & 1 \end{vmatrix}}{\begin{vmatrix} x_1 & 1 & y_1 & 1 \\ x_2 & 1 & y_2 & 1 \\ x_3 & 1 & y_3 & 1 \\ x_4 & 1 & y_4 & 1 \end{vmatrix}} = \frac{\begin{vmatrix} x_1 & y_1 & x_1 - x_2 \\ x_2 & y_2 & x_3 - x_4 \end{vmatrix}}{\begin{vmatrix} x_1 - x_2 & y_1 - y_2 \\ x_3 - x_4 & y_3 - y_4 \end{vmatrix}} \quad (3.7)$$

$$y = \frac{\begin{vmatrix} x_1 & y_1 & y_1 & 1 \\ x_2 & y_2 & y_2 & 1 \\ x_3 & y_3 & y_3 & 1 \\ x_4 & y_4 & y_4 & 1 \end{vmatrix}}{\begin{vmatrix} x_1 & 1 & y_1 & 1 \\ x_2 & 1 & y_2 & 1 \\ x_3 & 1 & y_3 & 1 \\ x_4 & 1 & y_4 & 1 \end{vmatrix}} = \frac{\begin{vmatrix} x_1 & y_1 & y_1 - y_2 \\ x_2 & y_2 & y_3 - y_4 \end{vmatrix}}{\begin{vmatrix} x_1 - x_2 & y_1 - y_2 \\ x_3 - x_4 & y_3 - y_4 \end{vmatrix}} \quad (3.8)$$

The intersection points of the two lines are computed by Eq.(3.7) and (3.8). By using these formulas intersection points of the lines are used to update grouped lines' starting and ending point coordinates. The results of line updating and grouping processes are given in Figure 17.



Figure 17 Grouped lines

The last step is to generate building borders from detected lines given in Figure 17. As explained before, the building detection strategy is based on L-shaped shadow detection method. So, two sides of the buildings have shadowed regions and two of them don't. Because of the region selection methodology, building borders far from the shadow region are not always selected and lines are not detected. This can be seen on Figure 17. Two buildings have lines only two sides of the building and the other sides are not detected. But because we are interested only rectangle buildings two sides of the buildings are enough to create rectangles around buildings. Also edge transitions around shadowed regions result line segments in the Hough transform stage. Because of this reason extracted line segments contain lines emerged from the shadowed regions.

In the last step the missing parts of the building line segments are generated by using geometrical relations. Because the opposite line segments are parallel to each other and have the same length, the missing parts are generated by using the opposite line segments. Figure 18 shows an example of line generation.

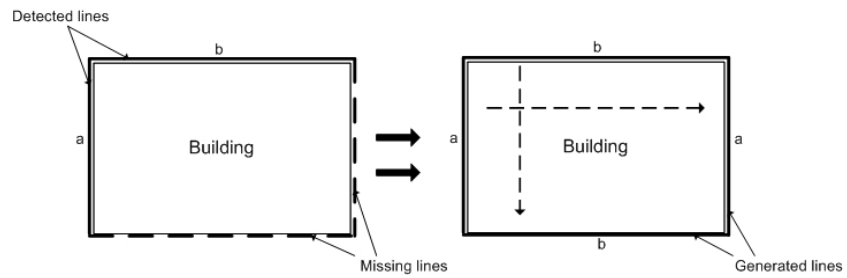


Figure 18 Line generation example

After missing parts of the lines are created, algorithm selects bigger rectangles over the buildings. This step is required because the algorithm produces too many lines in Hough transform stage due to start and finish angle thresholds. These thresholds can be set to ninety degrees to select only lines which intersect each other by ninety degrees. But this is not recommended in the practice because due to noise in the images or low resolution input images, building lines can not be detected by ninety degree precision and these lines are missed. So, selected rectangles are projected onto input image and results are given in Figure 19. The implemented algorithm steps are given in the next section and a flowchart is represented in Figure 20.



Figure 19 Detected Buildings

FLOWCHART OF THE LINE EXTRACTION AND BUILDING DETECTION

The procedural flowchart of the method is represented below:

- i. RGB image is converted to grayscale image.
- ii. Select shadowed regions from binary image.
- iii. Extract shadowed regions from grayscale image
- iv. Apply edge detection in the grayscale selected region image.
- v. Apply Hough Transform to extract (r,θ) pairs according to *Theta_res*.
- vi. Select (r,θ) pairs according to *Peak_Thr*
- vii. From selected (r,θ) pairs obtain line segments and remove smaller lines according to the *min_length* threshold.
- viii. Merge line segments according to *fill_gap* threshold.
- ix. Group extracted lines if the angles between lines are between *start* and *finish* and the distance is smaller than *dist_thr*.
- x. Intersect grouped lines according to Eq. (3.6) and (3.7) and update line segment start and ending point coordinates.
- xi. From grouped lines complete the missing border of the buildings.
- xii. Repeat until shadowed regions finishes.
- xiii. Plot bigger rectangles on the buildings.

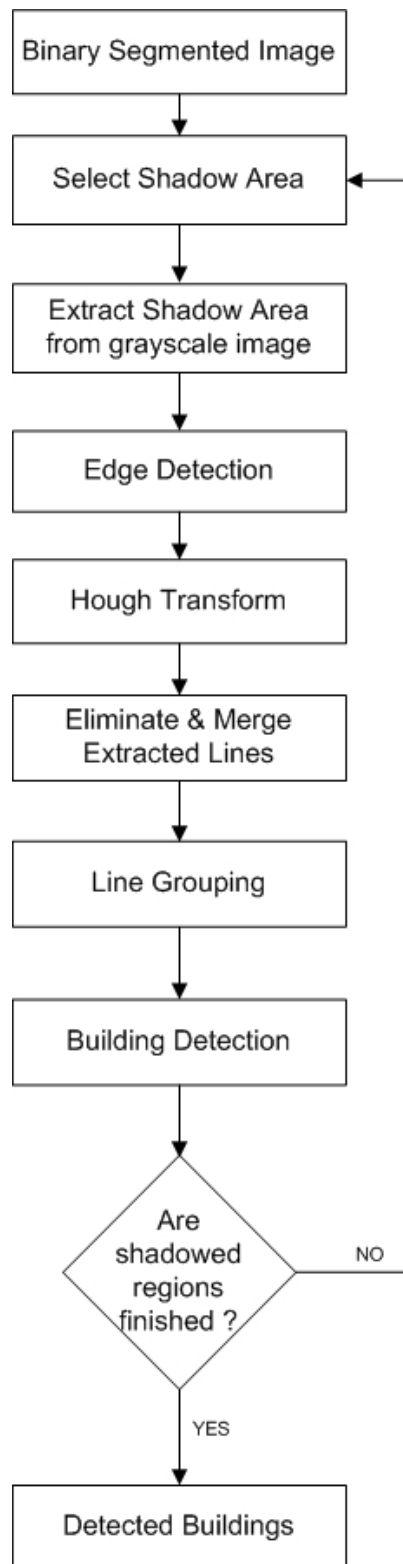


Figure 20 Basic Line Extraction and Building Detection Flowchart

3.4 MEAN SHIFT BASED BUILDING DETECTION

As mentioned in section 3.1 the mean shift segmentation output is used for building detection. In this study the algorithm implemented in [50] is used for image segmentation. The mean shift segmentation algorithm is applied on the image and result is given in Figure 21. As seen on the image, the segmentation output produces too much segments in the building roofs. So we need to find building roofs and re-segment these regions into one large segment.



a)

Mean Shift Segmented



b)

Figure 21 Mean Shift Result a) Original image b) Segmentation output

The implemented algorithm in [50] uses some parameters and these parameters are set before processing image. *MinimumRegionArea* controls the minimum cluster size, *SpatialBandWidth* controls segmentation spatial radius and *RangeBandWidth* controls segmentation feature space radius. These parameters are also explained in section 2.4.

Before processing segmented image, the implemented algorithm needs shadow direction as an input. All eight directions are accepted by the program. These directions are North, South, West, East, Northeast, Southeast, Southwest and Northwest. Image top section is assumed to be north, bottom is south, left part is west and right part is east.

The next step in the algorithm is region selection. This step is the same as Hough building detection method i.e. algorithm uses shadow image also. The algorithm selects shadow regions one by one and from shadow region boundaries, near clusters are searched in the opposite direction with respect to the shadow direction. Algorithm firstly selects the cluster near the shadow boundary. The first selected cluster is the main cluster in which other clusters will be added. By using this cluster, cluster boundaries are searched and similar clusters are added to the main clusters. The similarity measure is based on RGB value differences between selected cluster and main cluster. If percent difference (Eq.3.9) is below the threshold for all R, G, B bands then selected cluster is included in the main cluster. *THR* parameter is used for threshold value.

Each similar cluster is also checked if they exceed shadow boundaries or not. It is observed that some cluster regions exceed shadow boundaries somewhat. If exact shadow boundaries are used in the segmentation algorithm then these regions will be lost. So, shadow length is calculated and boundary regions are extended by some amount. *INC* parameter controls the increment ratio.

$$\%D i f f e r e n c e = \frac{|x_1 - x_2|}{\left(\frac{x_1 + x_2}{2}\right)} \times 100 \quad (3.9)$$

where x_1 is the R, G, B values of the selected cluster pixels and x_2 is the R, G, B values of the main cluster.

The algorithm stops searching when similarity threshold or shadow boundaries are exceeded for the selected region. By using segmented image as an input, the algorithm outputs are given in Figure 22 and Figure 23.



Figure 22 Detected Buildings



Figure 23 Building Borders

FLOWCHART OF THE MEAN SHIFT BASED BUILDING DETECTION

The procedural flowchart of the method is represented below:

- i. Input shadow direction (can be in all eight direction)
- ii. RGB image is segmented by using mean shift segmentation algorithm.
- iii. Select shadowed regions from previously found binary image.
- iv. By using shadow direction search pixels at the opposite direction in the segmented image
- v. Extract cluster boundaries from selected cluster.
- vi. Search selected cluster boundaries for similar clusters.
- vii. If the RGB values differences between the selected cluster and the other cluster is below *THR* then select this cluster as candidate cluster to be included.
- viii. Find boundaries of the candidate cluster.
- ix. If cluster boundaries exceed shadow boundaries more than $INC * \text{shadow length}$ then exclude selected cluster, if not then include selected cluster into main cluster.
- x. If shadow regions are finished then go to step xi, if not go to step iii.
- xi. Extract main segment boundaries for all selected regions and draw boundaries on the input image.

CHAPTER 4

IMPLEMENTATION AND RESULTS

4.1 INTRODUCTION

In this chapter implementation results of the proposed building detection method will be evaluated under different test images and effect of the shadow on building detection algorithms is investigated. Building detection algorithms firstly applied to shadowed images then shadowed removed images and results are compared. The test results are represented for nine different images. Buildings in the selected images differ in the means of orientation, building shapes, rooftop color contents and frequency of the buildings. In the previous chapters it is explained that the implemented algorithms focus on rectangular shaped buildings and assumed that these buildings have L-type shadows which surround two sides of the buildings. This assumption is taken into consideration in the image selection but also different building shapes are also used to determine algorithm efficiency. The data used in the algorithms consist of satellite images and Google Earth images. Satellite images are IKONOS satellite images with 1 m resolution taken from Eskisehir city. The detection results are given for both mean shift segmentation based building detection and Hough based building detection algorithms.

The performance of the implemented algorithm depends on image quality, image content, shadow occlusions, edge detector performance and shadow segmentation. Detailed explanations will be given in the following sections.

The algorithm is implemented on a computer which has Intel Pentium M 1.6 GHz processor and 512 MB RAM by using MATLAB software version R2008a.

4.2 PERFORMANCE ANALYSIS

The performances of the implemented algorithms will be compared based on the performance measures given in [16]. These are detection percentage (4.1) and branch factor (4.2).

$$\text{Detection Percentage} = 100 \times \frac{TP}{TP + TN} \quad (4.1)$$

$$\text{Branch Factor} = 100 \times \frac{FP}{TP + FP} \quad (4.2)$$

Here, TP is the number of buildings in the image which are detected by the algorithm, FP is the number of buildings detected by the algorithm which are not actually buildings and TN is the number of buildings in the image which are missed by the algorithm. In addition to these measures, two more measures are also used for performance evaluation: correctly labeled building pixels and incorrectly labeled building pixels. The accuracy of the extracted shape is measured by counting correct and non-correct building pixels. Correct building pixels percentage is calculated by the ratio of the number of correctly labeled building pixels over the number of building pixels in the image and incorrect building pixels percentage is calculated by the ratio of the number of incorrectly labeled pixels over the number of labeled building pixels [16].

In the above performance measures, a building is assumed to be detected if any part of the building is detected by the algorithms. The shape of the detected building may not necessarily be correct.

4.3 PARAMETER SELECTION

Both of the implemented algorithms use some parameters to be set. These parameters are given in Table 1. The effects of parameter selection on both algorithms are explained in this section with illustrations. Mean shift algorithm [50] parameters are also included in the mean shift based building detection algorithm parameters.

Table 1 Building Detection Parameters

Hough transform based building detection algorithm	<i>Theta_Res</i>	used for θ increment value.
	<i>Peak_Thr</i>	used for Hough Matrix peak selection.
	<i>Fill_Gap</i>	used for line merging distance.
	<i>Min_len</i>	Minimum line length
	<i>start</i>	line grouping starting angle
	<i>finish</i>	line grouping ending angle
	<i>dist_thr</i>	line grouping distance
Mean shift based building detection algorithm	<i>MinimumRegionArea</i>	Minimum cluster area
	<i>SpatialBandWith</i>	Segmentation spatial radius
	<i>RangeBandWith</i>	Segmentation feature space radius
	<i>INC</i>	Shadow boundary increment ratio.
	<i>THR</i>	Similarity measure between clusters

Hough transform uses some parameters and these parameters are explained in section 3.3. The algorithm efficiency depends on the parameter selection. As explained before, start and finish angles control which lines will be grouped according to the angles between them. If we use ninety degree precision, some of the detected lines will be excluded. This is illustrated in Figure 24.



Figure 24 Effect of *start* and *finish* parameters on Hough transform a) *start* and *finish* are set 90 deg b) *start* = 88, *finish* = 92

In Figure 24, first image is processed with *start* and *finish* parameters set to ninety degrees i.e. algorithm only searches ninety degree precision between detected lines. The output image shows that most of the buildings are missed. In the second image *start* and *finish* parameters are set to 88 and 92 degrees. So, it can be seen that, the building detection rate is increased.

In Figure 24, *Theta_Res* parameter is set to 1, which means θ values are incremented one by one. This will yield too many lines detected at the output of the Hough transform stage and also increases the sensitivity of the algorithm. To detect more buildings at the output, *Theta_Res* value is set to 2 and results are given in Figure 25.



Figure 25 Effect of *Theta_Res* parameter on Hough transform a) *Theta_Res*=1 b) *Theta_Res*=2

Also *Peak_Thr* parameter affects Hough transformation results at the beginning of the algorithm. Due to *Peak_Thr* parameter, peaks in the Hough matrix are selected and line segments are created. If this value is set to a higher value, than some of the peaks in the Hough matrix will not be selected and the pixels which have these peaks will not create line segments. This is illustrated in Figure 26. In the second image *Peak_Thr* is selected to be 0.7 which is higher than first image. So, in the output some of the buildings are missed, because of their lines are missed in peak selection stage.



Figure 26 Effect of *Peak_Thr* parameter on Hough transform a) *Peak_Thr*=0.4 b) *Peak_Thr*=0.7

Mean shift algorithm [50] used in Mean shift based building detection method also uses some parameters to detect buildings in the images. As explained in section 2.4 and 3.4 *MinimumRegionArea* controls minimum cluster size at the output. Increasing this value will remove small clusters at the rooftops, and generate homogeneous rooftop segments at the output. This is illustrated in Figure 27.

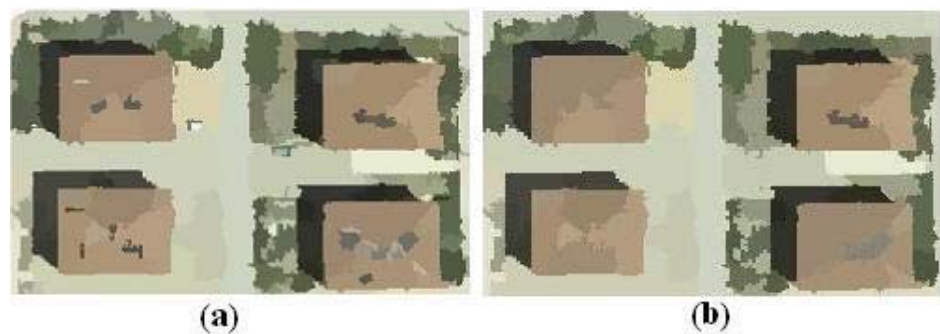


Figure 27 Effect of *MinimumRegionArea* parameter on Mean shift algorithm [50] a) *MinimumRegionArea*=15 pixels b) *MinimumRegionArea*=100 pixels

The other parameters in the algorithm, *SpatialBandWidth* and *RangeBandWidth*, also affect segmentation results. Increasing these values also increases kernel window sizes and this will cause cluster sizes to be increased and mean values are changed. This is illustrated in Figure 28.

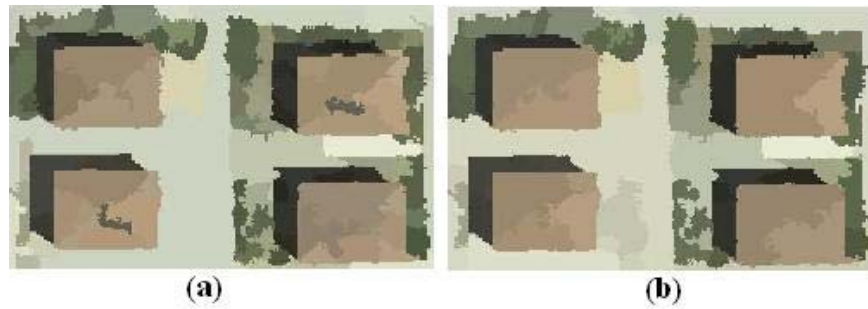


Figure 28 Effect of *SpatialBandwidth* parameter on Mean shift algorithm [50] a) *SpatialBandwidth*=5 b) *SpatialBandwidth*=10

The implemented Mean shift algorithm uses *THR* and *INC* parameters. These parameters are explained in section 3.4 also. If these values are selected smaller, the building borders will not be grouped as illustrated in Figure 29.



Figure 29 Effect of *THR* parameter on Mean shift based building detection algorithm a) *THR*=8 b) *THR*=15

Due to the complexity of the implemented algorithms, it is difficult to find theoretically optimal solutions. The parameter selection for test images is based on simplicity and intuitive judgements.

4.4 TEST RESULTS

The implemented algorithms are applied on 9 different images. 5 of the images are selected from IKONOS satellite image taken from Eskisehir city image. Other images are selected from Konya and Ankara cities on Google Earth software. In the first step, original images are processed with the algorithms and then shadow removed images are processed. In the implementation of shadow removed images, shadow image and shadow information is also known and used in the similar way with the original images. Selected images vary according to rooftop color contents, building shapes, orientation and building frequencies in the selected regions.

The first image is taken from Eskisehir. It is 298 x 203 pixels wide. The image (Figure 30) scene contains roads, trees, cars and lower right part is empty field. Buildings are separated from each other and surrounded by clear shadow regions. Figure 30 represents shadow information, shadow removed image and mean shift segmentation results. Figure 31 represents both building detection algorithm results and building detection results for test image #1 are given in Table 2.

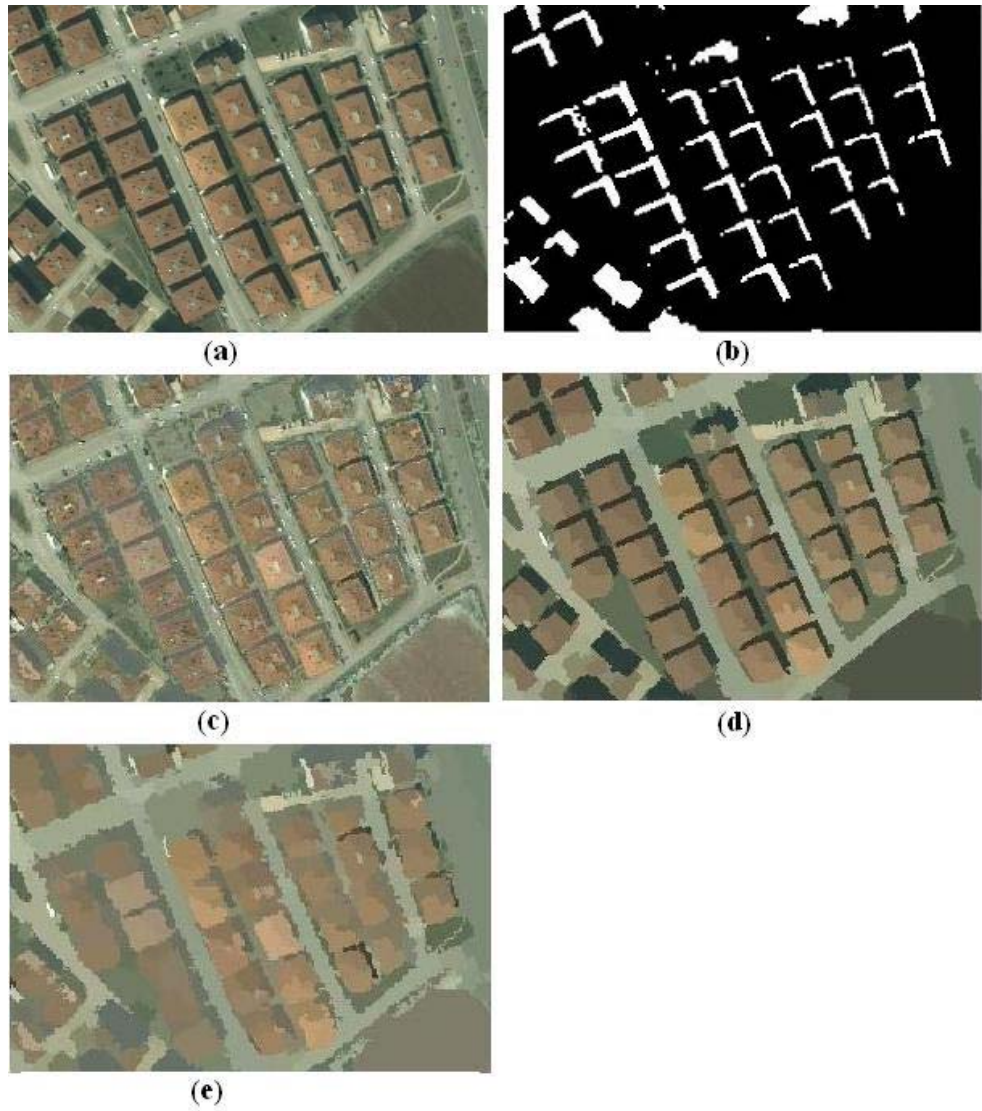


Figure 30 Test Results #1 a) Original image b) Shadow image c) Shadow removed image d) Mean shift segmented original image e) Mean shift segmented shadow removed image



Figure 31 Test Results #1 continued a) Detected buildings by Hough based detection algorithm on original image b) Detected buildings by Mean shift based detection algorithm on original image c) Detected buildings by Hough based detection algorithm on shadow removed image d) Detected buildings by Mean shift based detection algorithm on shadow removed image

Table 2 Image #1 Results

Detection Method	Branch factor	Detec. Perc.	cor.pix. perc.	incor. pix. perc.
Hough (original)	5%	87%	62%	25%
Hough (shadow removed)	16%	66%	60%	30%
Mean shift (original)	3%	97%	85%	2%
Mean shift (shadow removed)	12%	92%	65%	20%

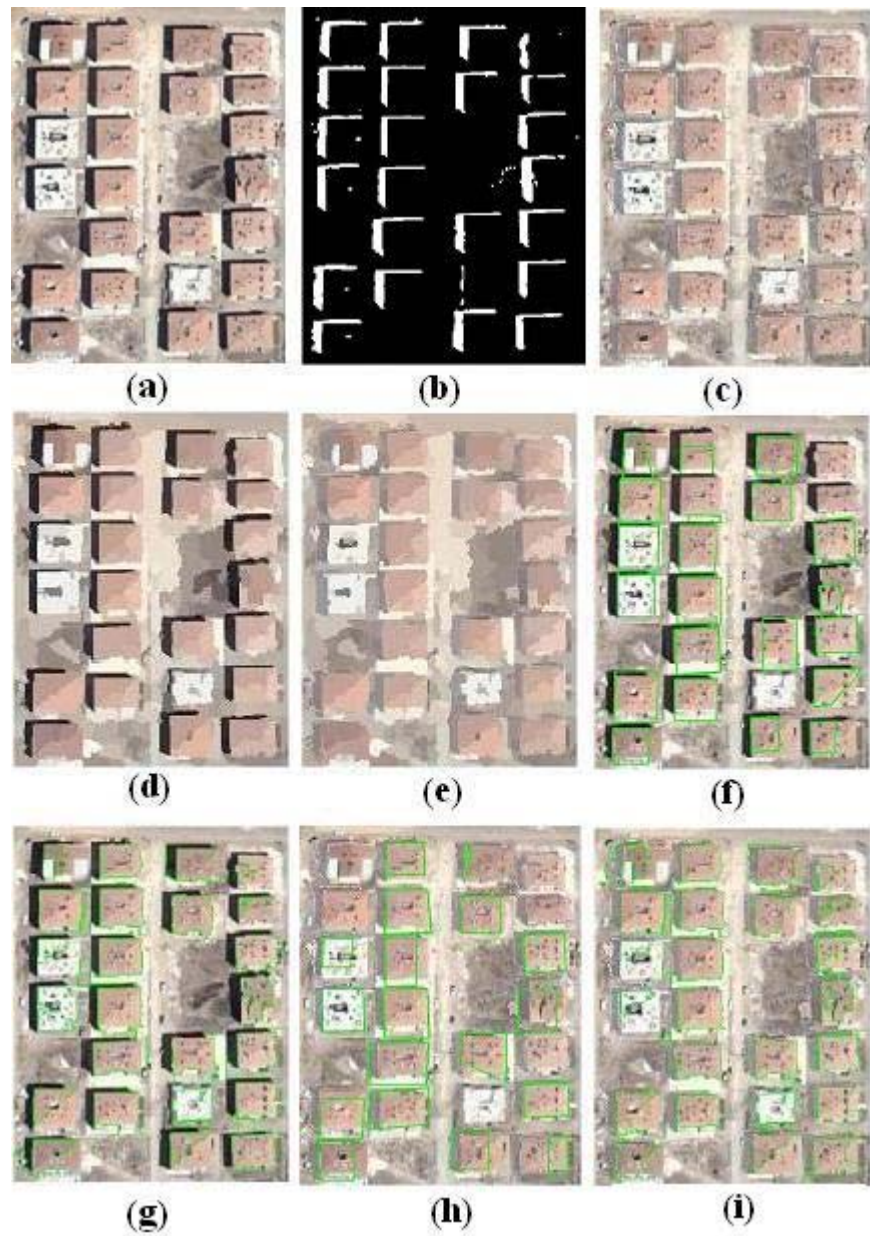


Figure 32 Test Results #2 a) Original image b) Shadow image c) Shadow removed image d) Mean shift segmented original image e) Mean shift segmented shadow removed image f) Detected buildings by Hough based detection algorithm on original image g) Detected buildings by Mean shift based detection algorithm on original image h) Detected buildings by Hough based detection algorithm on shadow removed image i) Detected buildings by Mean shift based detection algorithm on shadow removed image

Test image 2 is taken from Ankara city. It is 304 x 395 pixels wide. In Figure 32, buildings are separated from each other and surrounded by clear shadow regions. The rooftop colors and ground color are very similar. Three of the buildings have white colored rooftops on the other hand. The building detection results for both original image and shadow removed image are given in Table 3.

Table 3 Image #2 Results

Detection Method	Branch factor	Detec. Perc.	cor.pix. perc.	incor. pix. perc.
Hough (original)	4%	83%	71%	15%
Hough (shadow removed)	0	75%	63%	15%
Mean shift (original)	0	100%	82%	5%
Mean shift (shadow removed)	0	100%	78%	9%

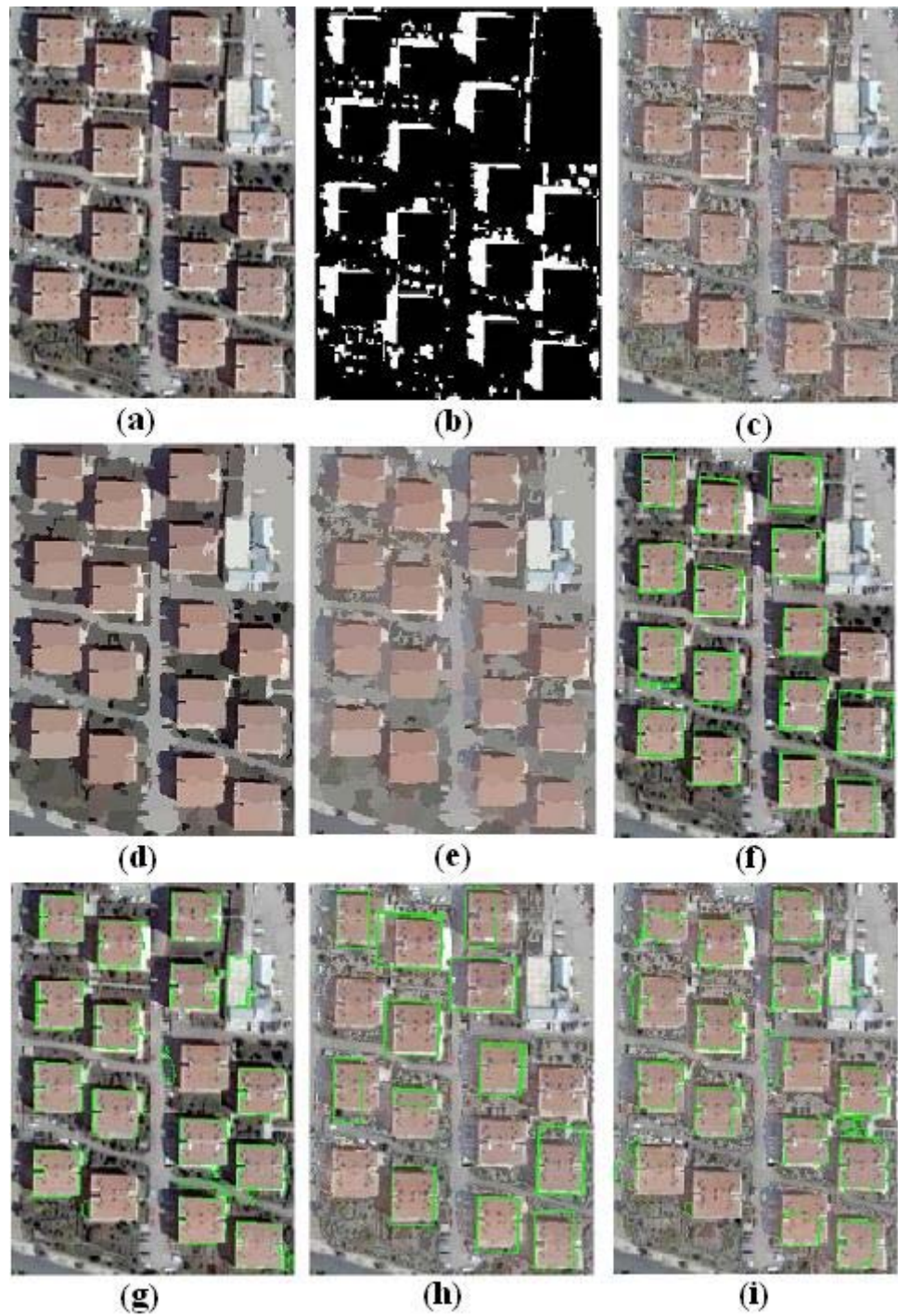


Figure 33 Test Results #3 a) Original image b) Shadow image c) Shadow removed image d) Mean shift segmented original image e) Mean shift segmented shadow removed image f) Detected buildings by Hough based detection algorithm on original image g) Detected buildings by Mean shift based detection algorithm on original image h) Detected buildings by Hough based detection algorithm on shadow removed image i) Detected buildings by Mean shift based detection algorithm on shadow removed image

Test image 3 is taken from Ankara city. It is 356 x 351 pixels wide. In Figure 33, selected region contains green fields and dark areas which result errors at the shadow detection algorithm. On the other hand buildings are separated from each other and surrounded by clear shadow regions. The rooftop colors are similar for all the buildings and building shapes are also rectangular. The building detection results for both original image and shadow removed image are given in Table 4.

Table 4 Image #3 Results

Detection Method	Branch factor	Detec. Perc.	cor.pix. perc.	incor. pix. perc.
Hough (original)	0	94%	85%	9%
Hough (shadow removed)	0	75%	84%	18%
Mean shift (original)	18%	87%	100%	0
Mean shift (shadow removed)	29%	75%	82%	0

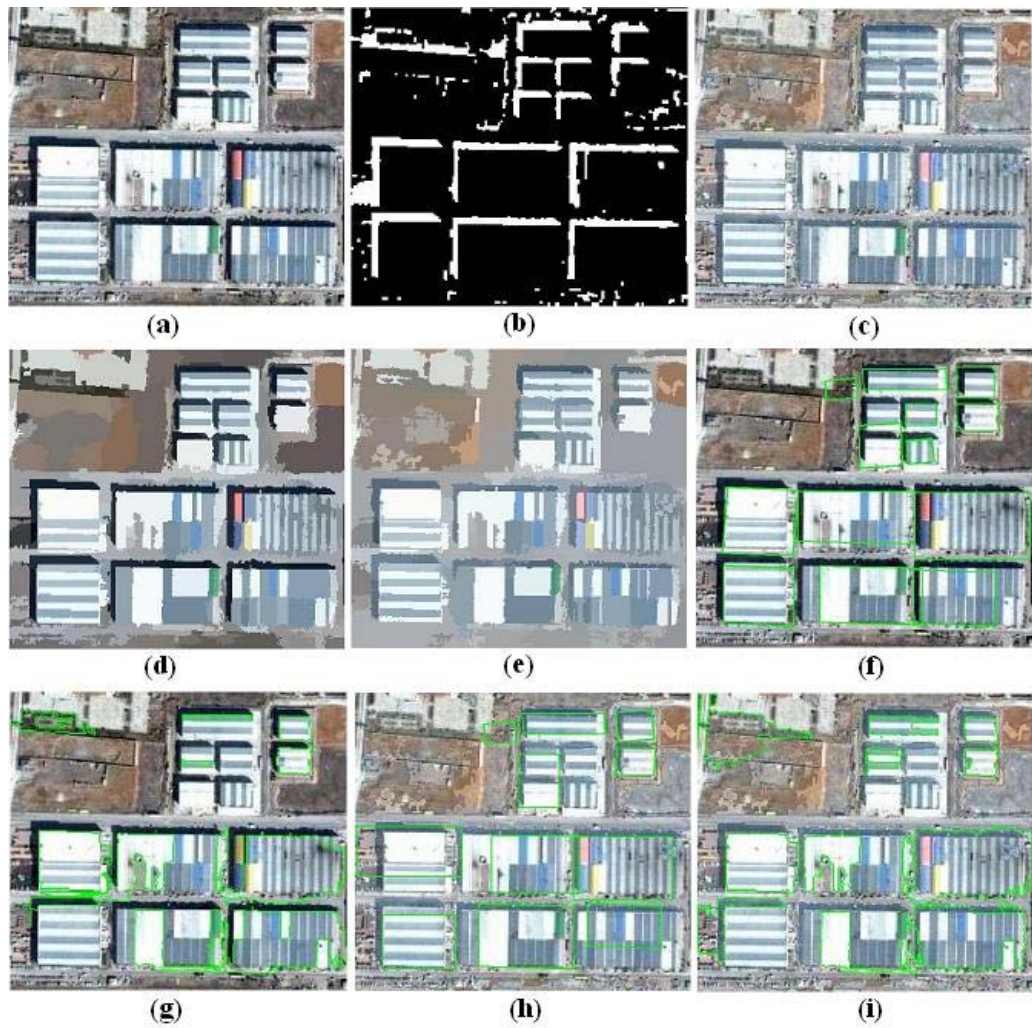


Figure 34 Test Results #4 a) Original image b) Shadow image c) Shadow removed image d) Mean shift segmented original image e) Mean shift segmented shadow removed image f) Detected buildings by Hough based detection algorithm on original image g) Detected buildings by Mean shift based detection algorithm on original image h) Detected buildings by Hough based detection algorithm on shadow removed image i) Detected buildings by Mean shift based detection algorithm on shadow removed image

Test image 4 (Figure 34) is taken from Konya city. It is 262 x 233 pixels wide. Building sizes are bigger than the first two images. Also building rooftops have different colors which make too many clusters at the mean shift segmentation output. To remove some of these clusters at the output, minimum region area and spatial bandwidth parameters (Table 13) are increased in the algorithm. In Figure 34 buildings are separated from each other and surrounded by clear shadow regions and building shapes are also rectangular. The building detection results for both original image and shadow removed images are given in Table 5.

Table 5 Image #4 Results

Detection Method	Branch factor	Detec. Perc.	cor.pix. perc.	incor. pix. perc.
Hough (original)	8%	92%	91%	15%
Hough (shadow removed)	9%	77%	82%	23%
Mean shift (original)	18%	69%	65%	5%
Mean shift (shadow removed)	18%	69%	73%	5%

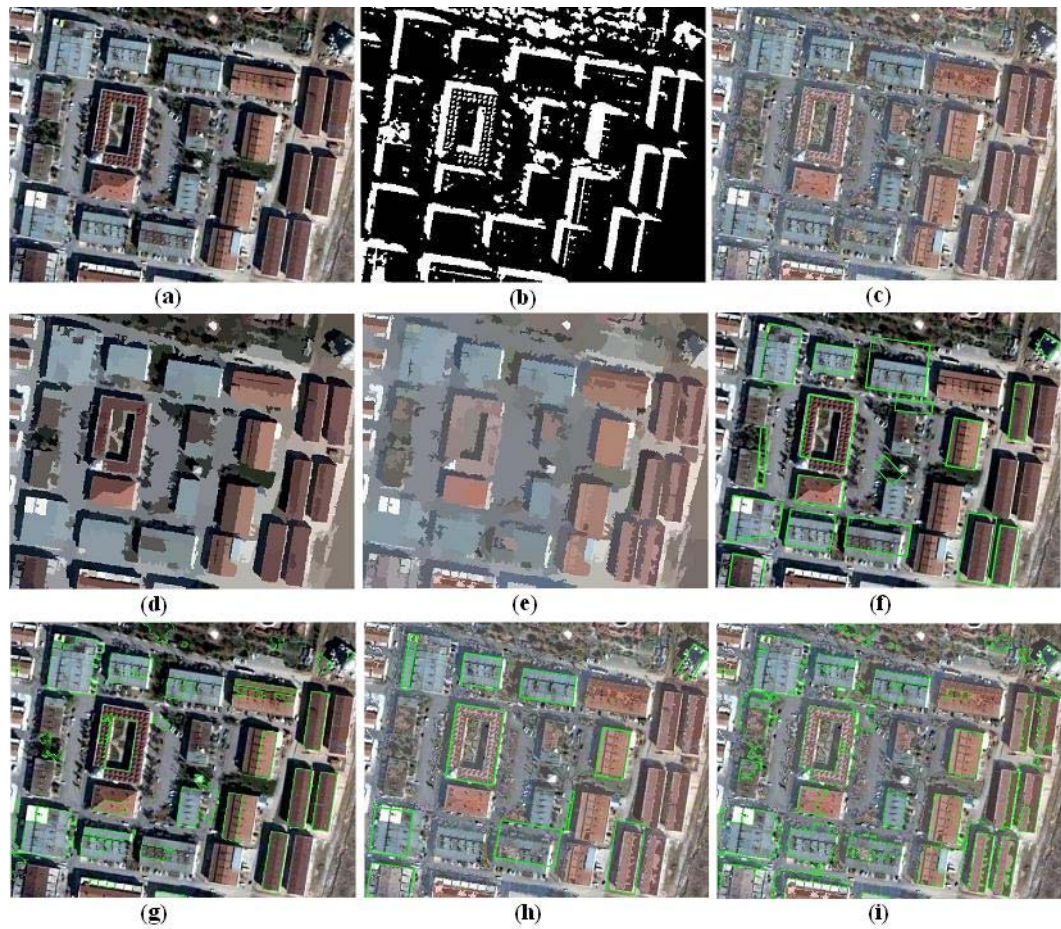


Figure 35 Test Results #5 a) Original image b) Shadow image c) Shadow removed image d) Mean shift segmented original image e) Mean shift segmented shadow removed image f) Detected buildings by Hough based detection algorithm on original image g) Detected buildings by Mean shift based detection algorithm on original image h) Detected buildings by Hough based detection algorithm on shadow removed image i) Detected buildings by Mean shift based detection algorithm on shadow removed image

Test image 5 (Figure 35) is also taken from Konya city. It is 453 x 360 pixels wide. Building sizes are different and different colored building rooftops exist in the image. Due to the non-homogeneity at the rooftops, minimum region area and spatial bandwidth parameters (Table 13) are also increased in the mean shift algorithm like we did in test image #4. Buildings are separated from each other

and surrounded by clear shadow regions and building shapes are also rectangular. But some spurious shadow regions are still exist in the image due to dark colored regions. The building detection results for both original image and shadow removed images are given in Table 6.

Table 6 Image #5 Results

Detection Method	Branch factor	Detec. Perc.	cor.pix. perc.	incor. pix. perc.
Hough (original)	17%	56%	91%	21%
Hough (shadow removed)	9%	40%	85%	14%
Mean shift (original)	36%	64%	68%	3%
Mean shift (shadow removed)	33%	88%	83%	6%

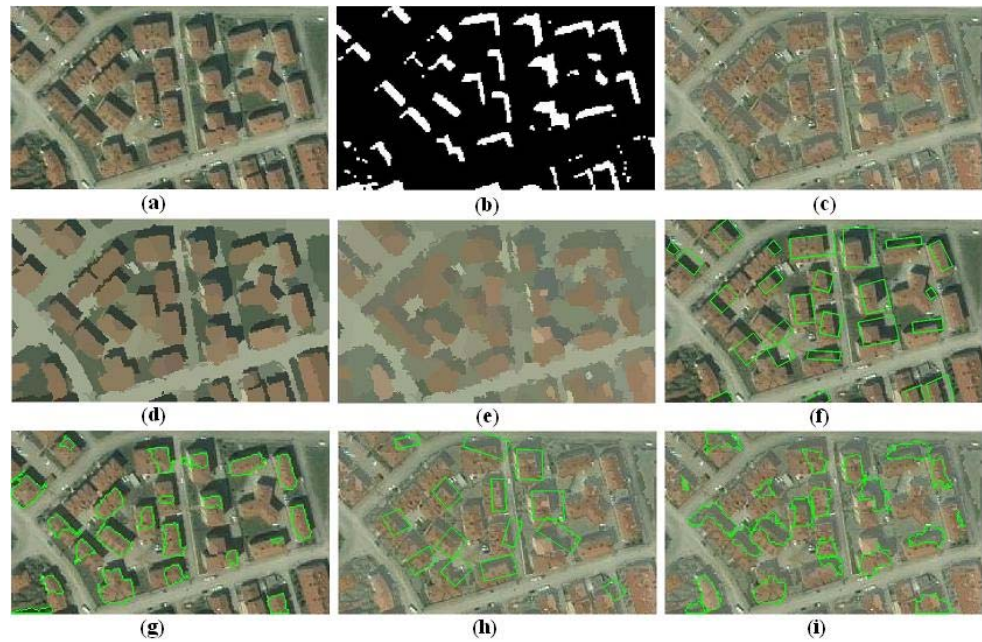


Figure 36 Test Results #6 a) Original image b) Shadow image c) Shadow removed image d) Mean shift segmented original image e) Mean shift segmented shadow removed image f) Detected buildings by Hough based detection algorithm on original image g) Detected buildings by Mean shift based detection algorithm on original image h) Detected buildings by Hough based detection algorithm on shadow removed image i) Detected buildings by Mean shift based detection algorithm on shadow removed image

Test image 6 (Figure 36) is taken from Eskisehir city. It is 236 x 136 pixels wide. Buildings have homogeneous rooftops and separated from each other. Building shapes are also rectangular but three building have different shapes. Also building orientations are different from each other. The building detection results for both original image and shadow removed images are given in Table 7.

Table 7 Image #6 Results

Detection Method	Branch factor	Detec. Perc.	cor.pix. perc.	incor. pix. perc.
Hough (original)	36%	59%	78%	22%
Hough (shadow removed)	35%	33%	71%	15%
Mean shift (original)	5%	77%	92%	3%
Mean shift (shadow removed)	45%	44%	68%	8%

Test image 7 (Figure 37) and test image 8 (Figure 39) are taken from Eskisehir city. Buildings have homogeneous rooftops in the images. Building shapes are also rectangular but some of the buildings have different shapes. Building sizes and frequencies in the images are varying. The building detection results for both original image and shadow removed images are given in Table 8, Table 9.

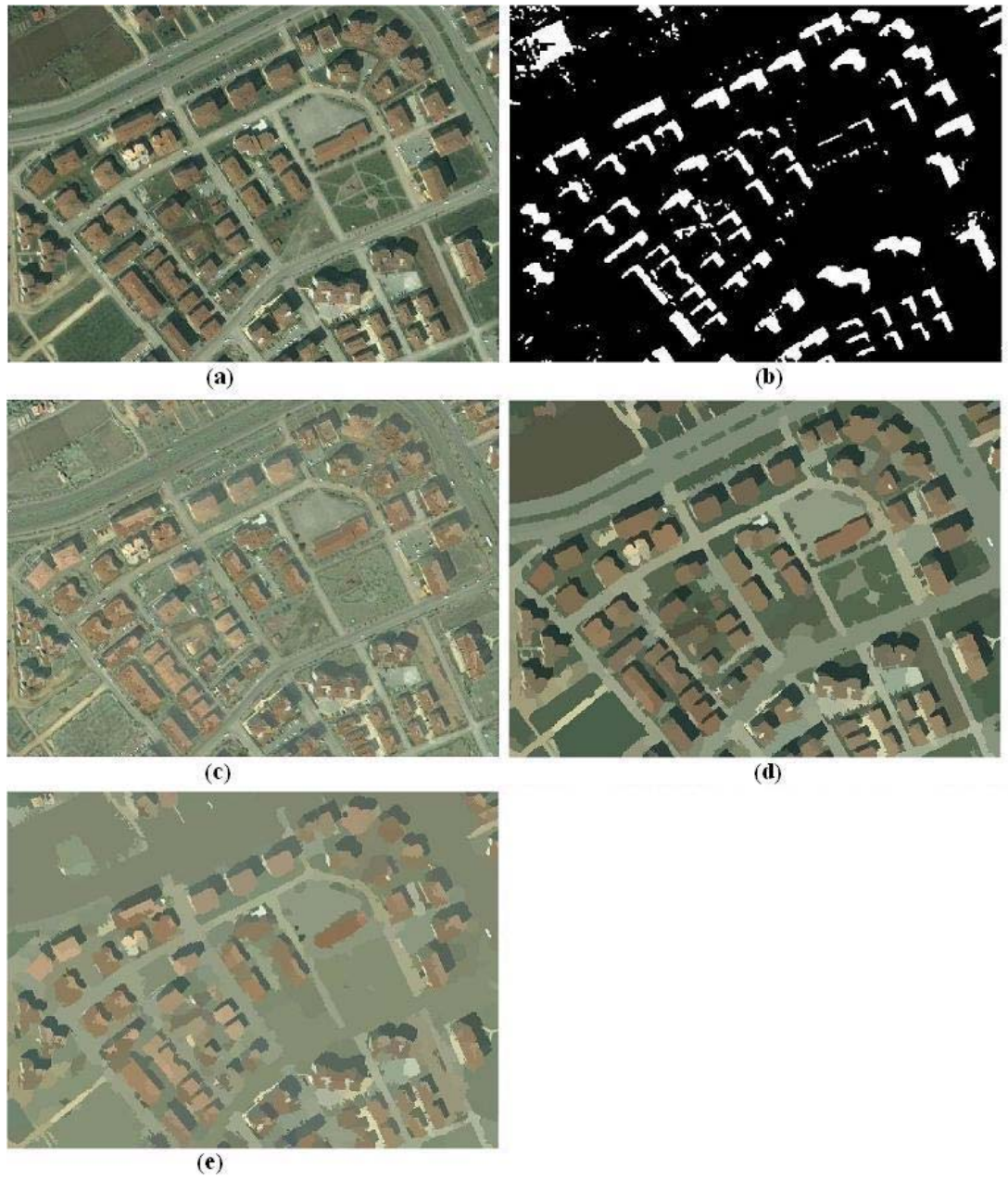


Figure 37 Test Results #7 a) Original image b) Shadow image c) Shadow removed image d) Mean shift segmented original image e) Mean shift segmented shadow removed image



Figure 38 Test Results #7 continued a) Detected buildings by Hough based detection algorithm on original image b) Detected buildings by Mean shift based detection algorithm on original image c) Detected buildings by Hough based detection algorithm on shadow removed image d) Detected buildings by Mean shift based detection algorithm on shadow removed image

Table 8 Image #7 Results

Detection Method	Branch factor	Detec. Perc.	cor.pix. perc.	incor. pix. perc.
Hough (original)	19%	48%	62%	27%
Hough (shadow removed)	27%	43%	80%	17%
Mean shift (original)	19%	84%	86%	5%
Mean shift (shadow removed)	29%	68%	76%	8%

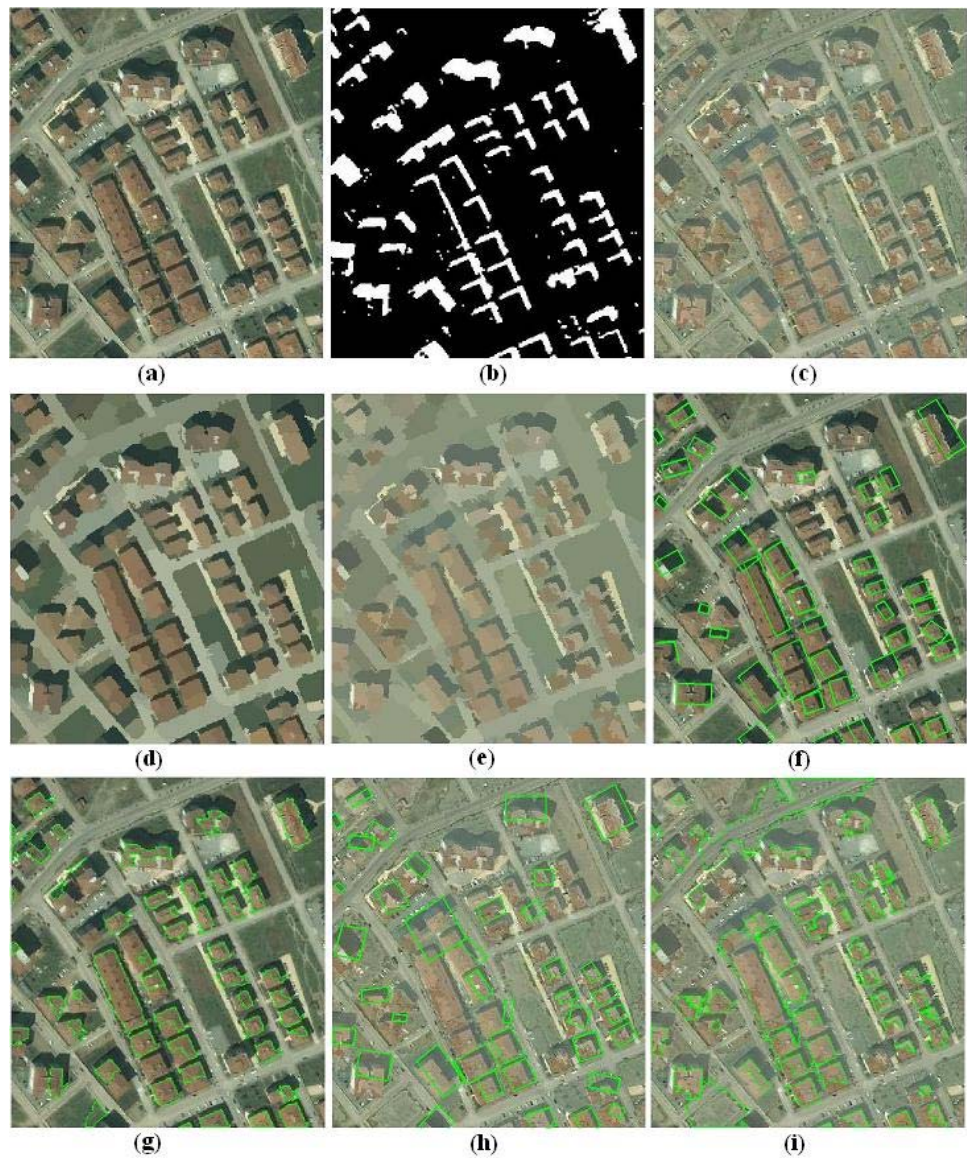


Figure 39 Test Results #8 a) Original image b) Shadow image c) Shadow removed image d) Mean shift segmented original image e) Mean shift segmented shadow removed image f) Detected buildings by Hough based detection algorithm on original image g) Detected buildings by Mean shift based detection algorithm on original image h) Detected buildings by Hough based detection algorithm on shadow removed image i) Detected buildings by Mean shift based detection algorithm on shadow removed image

Table 9 Image #8 Results

Detection Method	Branch factor	Detec. Perc.	cor.pix. perc.	incor. pix. perc.
Hough (original)	23%	63%	73%	27%
Hough (shadow removed)	27%	55%	69%	32%
Mean shift (original)	8%	90%	84%	7%
Mean shift (shadow removed)	10%	90%	70%	13%

Test image 9 (Figure 40) is also taken from Eskisehir city. It is 304 x 348 pixels wide. Building sizes are different and buildings are very closer to each other. Buildings have homogeneous rooftops in the images. Building shapes are also rectangular. The building detection results for both original image and shadow removed images are given in Table 10.

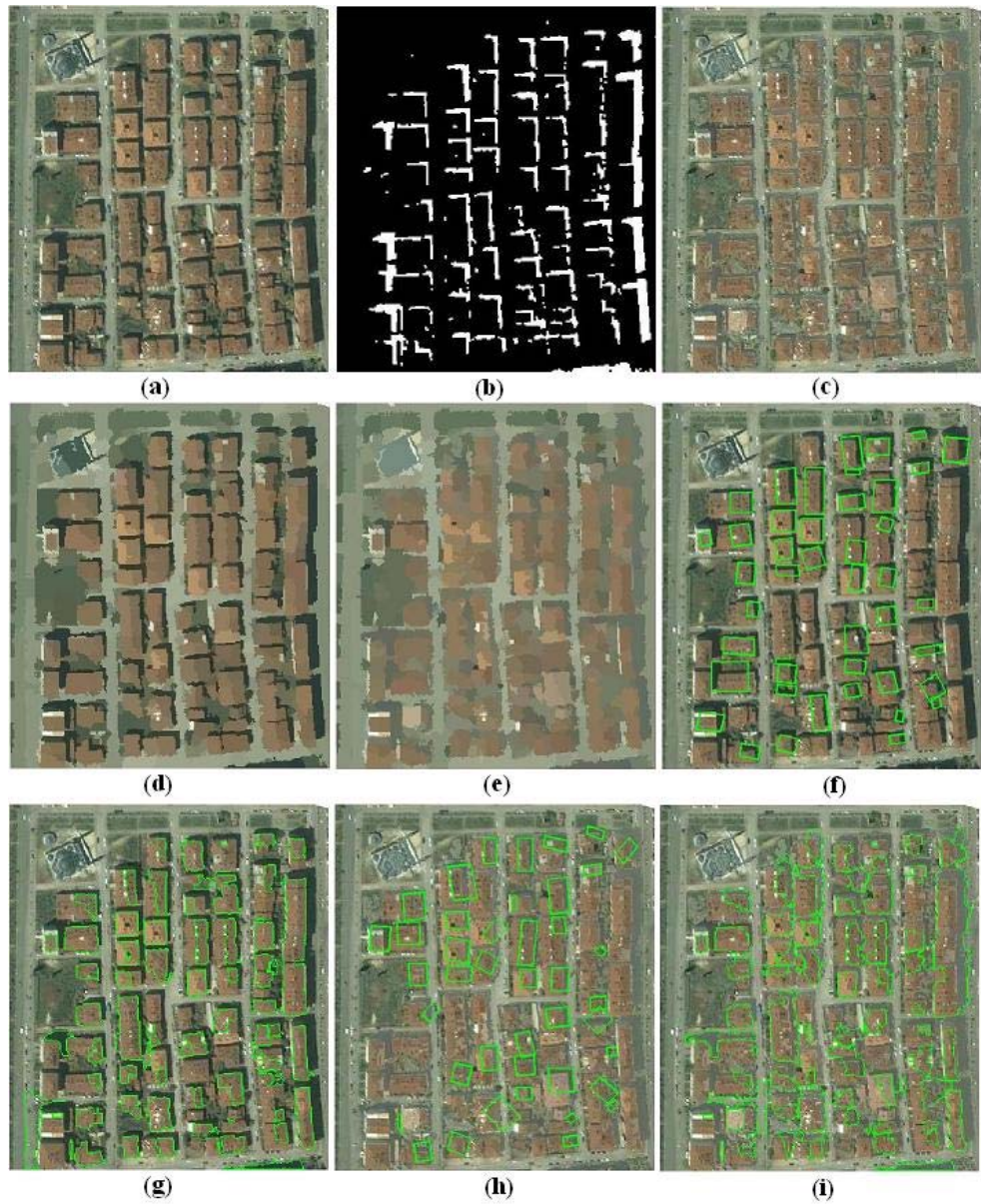


Figure 40 Test Results #9 a) Original image b) Shadow image c) Shadow removed image d) Mean shift segmented original image e) Mean shift segmented shadow removed image f) Detected buildings by Hough based detection algorithm on original image g) Detected buildings by Mean shift based detection algorithm on original image h) Detected buildings by Hough based detection algorithm on shadow removed image i) Detected buildings by Mean shift based detection algorithm on shadow removed image

Table 10 Image #9 Results

Detection Method	Branch factor	Detec. Perc.	cor.pix. perc.	incor. pix. perc.
Hough (original)	9%	56%	77%	19%
Hough (shadow removed)	20%	46%	68%	15%
Mean shift (original)	9%	84%	86%	5%
Mean shift (shadow removed)	18%	78%	75%	18%

For all nine test images, building detection results are represented in Table 11 and Table 12.

Table 11 Hough transform based building detection algorithm results

Image	Hough transform based building detection algorithm							
	Original Image				Enhanced image			
	Branch factor	Det. perc.	cor. pix perc.	incorr. pix. perc.	Branch factor	Det. perc.	cor. pix perc.	incorr. pix. perc.
#1	5%	87%	62%	25%	16%	66%	60%	30%
#2	4%	83%	71%	15%	0	75%	63%	15%
#3	0	94%	85%	9%	0	75%	84%	18%
#4	8%	92%	91%	15%	9%	77%	82%	23%
#5	17%	56%	91%	21%	9%	40%	85%	14%
#6	36%	59%	78%	22%	35%	33%	71%	15%
#7	19%	48%	62%	27%	27%	43%	80%	17%
#8	23%	63%	73%	27%	27%	55%	69%	32%
#9	9%	56%	77%	19%	20%	46%	68%	15%

Table 12 Mean shift based building detection algorithm results

Image	Mean shift based building detection algorithm							
	Original Image				Enhanced image			
	Branch factor	Det. perc.	cor. pix perc.	incorr. pix. perc.	Branch factor	Det. perc.	cor. pix perc.	incorr. pix. perc.
#1	3%	97%	85%	2%	12%	92%	65%	20%
#2	0	100%	82%	5%	0	100%	78%	9%
#3	18%	87%	100%	0	29%	75%	82%	0
#4	18%	69%	65%	5%	18%	69%	73%	5%
#5	36%	64%	68%	3%	33%	88%	83%	6%
#6	5%	77%	92%	3%	45%	44%	68%	8%
#7	19%	84%	86%	5%	29%	68%	76%	8%
#8	8%	90%	84%	7%	10%	90%	70%	13%
#9	9%	84%	86%	5%	18%	78%	75%	18%

For all nine images, the parameters used in the algorithms and computation times are given in Table 13 and Table 14.

Table 13 Algorithm parameters used in the images

Parameters	Test Images								
	#1	#2	#3	#4	#5	#6	#7	#8	#9
<i>Theta_Res</i>	2	2	1	2	1	3	1	2	3
<i>Peak_Thr</i>	0.4	0.4	0.6	0.4	0.4	0.3	0.4	0.4	0.4
<i>Fill_Gap</i>	10	10	10	15	10	15	15	15	10
<i>Min_len</i>	2	2	2	2	2	2	2	2	2
<i>start</i>	88	88	88	88	88	85	85	85	85
<i>finish</i>	92	92	92	92	92	95	95	95	95
<i>dist_thr</i>	10	10	10	10	10	15	15	15	15
<i>Minimum RegionArea</i>	15	15	15	50	50	15	15	15	15
<i>Spatial BandWith</i>	7	7	7	15	15	7	7	7	7
<i>Range BandWith</i>	6.5	6.5	6.5	6.5	6.5	6.5	6.5	6.5	6.5
<i>INC</i>	0.2	0.2	0.35	0.2	0.2	0.35	0.35	0.35	0.30
<i>THR</i>	20	20	18	40	30	18	18	18	18

Table 14 Run Time Evaluations

Test Images	Image Size	Total Run Time
#1	298x203	28 sec.
#2	304x395	36 sec
#3	256x351	32 sec
#4	262x233	30 sec
#5	453x360	126 sec
#6	236x136	15 sec
#7	522x379	140 sec
#8	305x341	63 sec
#9	304x348	70 sec.

From Table 11 and Table 12, average building detection results are given in Table 15.

Table 15 Average building detection results

Algorithm	Original Image				Shadow Removed Image			
	Branch factor	Det. perc.	cor. pix perc.	incorr. pix. perc.	Branch factor	Det. perc.	cor. pix perc.	incorr. pix. perc.
Hough	13%	71%	77%	20%	16%	57%	74%	20%
Mean shift	13%	84%	83%	4%	22%	78%	74%	10%

4.5 EVALUATION OF THE RESULTS

In Table 15, it is observed that, best results are achieved by mean shift based building detection algorithm. Because the dependency of L-type shadow regions, Hough based building detection algorithm has failed in some regions where L-shaped shadow is not available. Most of the buildings have L-shaped shadow regions but during morphological cleaning operations to remove spurious regions, some of L-shape shadow regions lost their shape and makes building detection impossible by Hough based building detection algorithm. This is illustrated in Figure 41 for test image #2 in Figure 32. Shadow regions numbered with #1 and #2 are not detected in the Hough detection based building detection method.

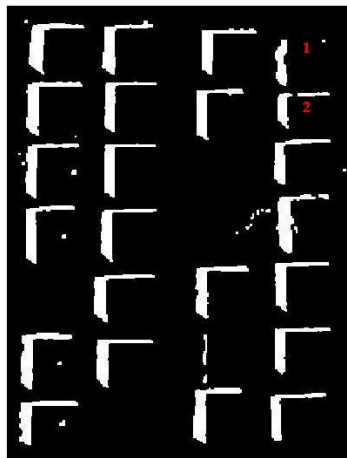


Figure 41 Lost L-shape shadow regions

Since Mean shift based building detection algorithm uses shadow direction and searches shadow boundaries cluster by cluster, it detects some regions in these shadow regions where L-shape structure is not available. In Figure 32 g) it can be

seen that, mean shift based building detection algorithm detects some regions on shadow region #1 and #2 in Figure 41.

But due to the high amount of green fields in the image, shadow detection algorithm detected these regions as shadow areas and made shadow areas non-uniform in Figure 33. Due to the mechanism of the mean shift based building detection algorithm, it starts searching from shadow boundaries, and found clusters where non-shadow building areas are detected. But in non-uniform shadow regions, there exist some small gaps in the shadow boundaries and when the algorithm starts it will stop when non-shadow areas are detected and this will cause false positives at the output. This is illustrated in Figure 42. In shadow regions #1 and #2, because the shadow boundaries are not uniform, false positives are appeared in the boundaries of these regions.

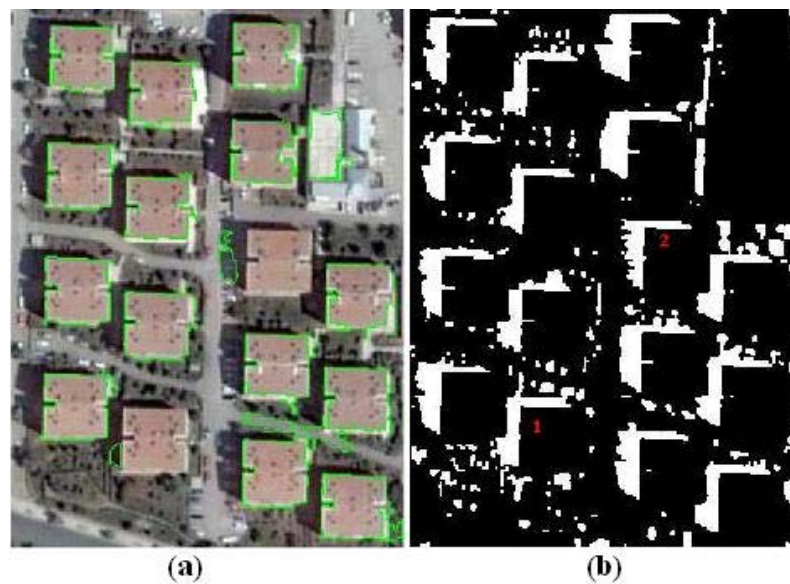


Figure 42 False positives due to non-uniform shadow regions at the output of the mean shift based building detection algorithm

For test image #1, #2, #3 and #4 Hough based building detection algorithm performed well but not as good as mean shift based building detection algorithm. Because of the scene simplicity and existence of L-shape shadow region, most of the buildings are detected at the output. Also the algorithm parameters are same for test image #1 and #2 and only *fill_gap* parameter is different in test image #4. But when the scene complexity is increased, algorithm has started to perform worst. In test image #5, results went worse because of the increase in the non-uniform and not clear shadow areas. Due to the sizes of the buildings, building orientations non-clear shadow areas and building shapes, Hough transform results are worse than the first four test images in test images #6, #7 and #8. For test image #6, #7 and #8, some of different shaped building structures are detected but the extracted rectangles do not cover full shape due to the nonexistence of L-shape shadow areas. Also scene complexity made parameter detection hard to determine for test image #6, #7 and #8. In test image #9 a different area is selected where buildings are very close to each other and building boundaries and shadow areas are barely detectable. Because of the buildings are very close to each other, and different sized building structures, it is hard to determine Hough transform parameters.

Mean shift segmentation algorithm performed better than Hough transform based building detection algorithm where shadow areas are clear and uniform. Non-uniform shadow areas, and dark colored areas in the images results false positives at the output. Also different color contents in the rooftops causes worse results at the output which is given in Figure 34. In test image #4, rooftops have non-homogeneous color contents and this result too many clusters at the mean shift segmentation algorithm output. To remove some of these regions, *minimum region area* and *range bandwidth* parameters are selected to be larger values. But at the output results are not as good as Hough based building detection algorithm. On the other hand; scene complexity, building frequencies in the images, different building sizes and different building shapes do not affect building detection results. *INC* and *THR* parameters are easy to set and achieve encouraging results. By mean shift segmentation, better results are achieved than Hough transform based building detection algorithm. The detection results are given in Table 12.

In the last step, both algorithms are applied to shadow removed images. In the shadow removal algorithm, each shadow region boundaries are found and surrounding mean R, G and B values are stored in shadow regions by linear correlation technique. By storing shadow boundary RGB values into shadowed regions, shadow and building rooftop transition is smoothed in shadow removal algorithm and building boundaries are lost at the output images. Although Hough transform needs clear edges, the shadow removal algorithm smoothes these regions and some edges are lost during shadow removal process. This causes buildings are not detected by the algorithm. Also new edges arose in the output due to threshold change in canny edge detector. In the implemented algorithm Canny edge detector thresholds are determined automatically over the test image by looking gradient changes. But when we changed shadow areas to non-shadow areas, the gradient changes are removed for shadow areas and new threshold values obtained. The difference between original edge image and shadow removed edge image is illustrated for test image #1 in Figure 43.

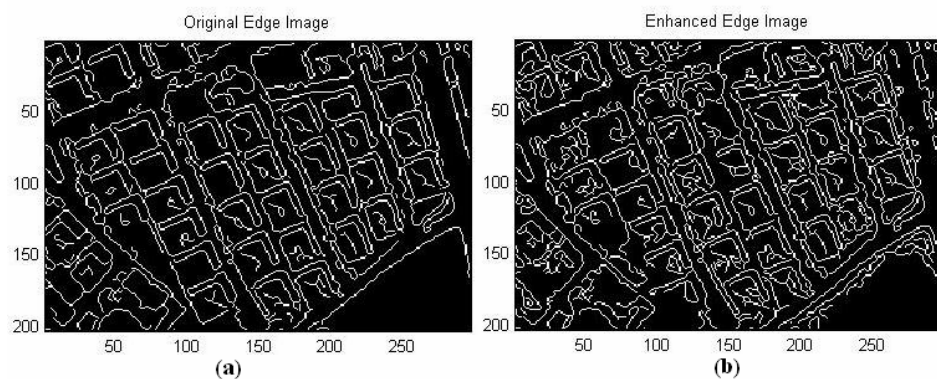


Figure 43 Edge Image Comparison for test image #1 a) Original edge image b) Shadow removed edge image

Same problems also occurred in the mean shift based building detection algorithm. By storing surrounding RGB values into shadow regions, mean values of these regions are converged to the means of the surroundings. At the clustering stage of the mean shift algorithm, these shadow removed regions are clustered with nearby clusters (building rooftop clusters) and cluster sizes are increased. This increase can be tolerated by some amount by decreasing *INC* parameter which increases shadow boundaries to be passed. But decreasing this value reduces the detected building areas at the output. An example is given for test image #1 in Figure 44.



Figure 44 Mean shift based building detection outputs a) by using original image b) by using shadow removed image

If we compare average results in Table 15, we will see that mean shift based building detection algorithm performs better than Hough based building detection algorithm. Only branch factor value for shadow removed image is higher than Hough based algorithm. This result comes from the over segmentation of shadow removed areas with building boundaries. When algorithm starts to search non-shadow areas around shadow boundaries in the opposite direction with respect to the shadow direction if non shadowed region is found then algorithm labels this

regions as building regions. This is true indeed but because of labeled region is very close to shadow removed area it is clustered together with this region in the mean shift clustering step. Because the selected region contains small areas on the buildings and large areas on the outside of the buildings, selected region is labeled as false positives and increased branch factor value.

On the other hand other parameters are better for mean shift segmentation algorithm. Because of scene complexity, different building orientations and building frequencies, Hough transform results are worse than mean shift algorithm.

CHAPTER 5

DISCUSSION AND CONCLUSION

5.1 SUMMARY

In this study, shadow based building detection methods are implemented for two different algorithms. These methods uses shadow presence as an evidence for buildings. The proposed algorithms are used for rectangular-shaped building detection.

In the first step shadow segmentation is performed and shadow image is obtained. By using shadow images, shadow areas are removed from the images. Both original and shadow removed images are processed with the implemented algorithms. For building detection, Hough based and mean shift based building detection methods are implemented. Hough transform based building detection method is based on the assumption of L-shaped shadow areas around buildings. Mean shift based building detection algorithm uses both shadow information and mean shift segmented image for building detection. The implemented algorithms are performed for nine different images which have different type of shadows, building size, building types and building frequencies.

5.2 DISCUSSION

The proposed building detection method has two main parts. First one is the shadow segmentation part. The shadow segmentation part is performed well for most of the images but resulted false positives where dark colored areas exist in the

image. Main contents of these areas are green fields and trees. These areas can be removed by increasing Otsu threshold. Increasing Otsu threshold removes false positives in the image but weakens the shadowed region connectivity. Too much increase in the threshold will cause L-shaped shadow regions to be removed from the image and produces lower detection results at the building detection output. Also the morphological operations are used to remove small spurious regions to increase efficiency. But increasing the window size will also weaken shadowed region connectivity.

The second main part is building detection methods. These methods are Hough transform based and mean shift segmentation based building detection algorithms.

In Hough transform based building detection algorithm, Canny edge detection algorithm is used to detect building edges. Edge detection part plays main role in Hough transform because lines are extracted by using edge points. If the edge detector algorithm performance is better than Hough transform also produces better results. Also the image quality will affect edge detector performance and line extraction stage. High resolution images contain detailed information and give too many edges at the edge detector output. But in less detailed images some edges are not detected due to noise and this will result building lines not to be detected by the algorithm.

The edge detector output is used in the line extraction stage. The line extraction step uses Hough transform to detect line segments. The algorithm needs some parameters to be adjusted before the algorithm runs. These parameters play key roles in the algorithm. Because the algorithm is highly dependent on these parameters, the detection results vary according to the images. It has been observed that implemented algorithm produces better results in separated building areas and uniform building shapes. Although the implementation complexity of Hough transform, by using L-shape shadow regions, only the selected region is performed and algorithm computation time is lowered and some false positives are also removed.

In mean shift segmentation based building detection algorithm, image is first segmented into clusters by using mean shift segmentation algorithm. Mean shift segmentation algorithm uses three parameters and two of these parameters are changed in the implementations. For buildings which have non-uniform building rooftops minimum region area and spatial bandwidth parameters are increased to smooth non-uniform building rooftops. If these parameters are chosen to be a larger value then, the cluster sizes will increase and image details will be lost. The building detection method uses segmented image and shadow direction as an input. Each shadow areas extracted at first. Given the shadow direction similar clusters are grouped in the opposite direction to shadow boundaries. Similar clusters are grouped according to some rules. If RGB value differences between selected cluster and its neighbour clusters are below the given threshold, then these clusters are selected as candidate clusters to be grouped. Before grouping candidate clusters, each cluster boundaries are checked whether they exceed shadow boundaries or not. In some regions building rooftop and ground segments have very similar color contents and they can be grouped if we check only threshold values. Test results show that some clusters around shadow boundaries can exceed shadow boundaries by some amount in the segmented image. So, if we use exact shadow boundaries, clusters around shadow boundaries will not be grouped. Because of this reason, INC threshold value is used to increment shadow boundaries by some amount and include boundary clusters.

In the last step, each shadow regions are removed from image. These regions are selected one-by one and from shadow boundaries a mean value is calculated. Calculated mean value is then stored in shadow regions by linear correlation. After all the shadow regions are removed, these images are applied to building detection algorithms. Test results showed that some edges are lost during the shadow removal algorithm. Because of Hough transform needs edges to extract line segments; the algorithm is unable to detect these line segments. A different problem is occurred in the mean shift algorithm also. When we store boundary mean RGB values into shadow regions, they tend to be clustered with boundary clusters which also include

rooftop clusters. It is observed that boundary loss and over segmentation effects lowers the detection rate and increases false positives at the output.

So, it is observed that mean shift segmentation algorithm produces better results than Hough transform based building detection algorithm. Because of Hough transform uses some geometrical relations to detect line segments and angle values in the line grouping part, parameter selection and edge detection plays main roles in the outputs. In some regions where building sizes, building orientations and building frequencies are different, it is hard to set these parameters without trial and error. On the other hand, mean shift parameters are easier to set than Hough transform parameters.

Also, it is shown that shadow removal algorithm performs very fast and results are encouraging but it is not applicable for proposed building detection algorithms due to the given problems.

Finally, the implemented algorithms depend on some parameters and these parameters vary according to the selected image. By adjusting these parameters efficiently, the performance of the algorithms can be improved.

5.3 FUTURE WORK

A first step forward from this work is to detect different types of building shapes rather than rectangular, such as circular, pentagonal and hexagonal types. The building shadows can be used to detect building heights and from this information 3-D models of the buildings can be generated.

Because of the implemented algorithms are using shadow information, shadow detection algorithm can be improved by using vegetation index of the image. This can be extracted from different data sources.

Although shadow information is extracted from images, it is not used in the line selection part of Hough transform. Detected lines are grouped according to the angles between them. But in some regions lines in the shadow areas are also selected when they satisfy certain conditions. By using shadow information, detected shadow lines can be removed from the results and true building regions can be extracted.

Shadow direction is needed for mean shift based building detection algorithm but although the shadow regions are clearly extracted, some geometrical relations can be used to extract shadow direction automatically from the image without user interaction.

The proposed algorithms highly depend on parameters. By changing these parameters, the performance of the algorithms can be improved. The automation in parameter selection will decrease user-dependency.

REFERENCES

- [1] Levitt S., Aghdasi F., “Moving Toward A Learning Fuzzy Building Recognition System”, Knowledge-Based Intelligent Information Engineering Systems, Third International Conference Volume , Issue , Dec 1999, Page(s):268 – 271
- [2] Noronha S., Nevatia R., “Detection and Description of Buildings from Multiple Aerial Images”, IEEE Computer Society Conference on Computer Vision and Pattern Recognition (CVPR'97), 1997, pp.588
- [3] Krishnamachari S., Chellappa R., “Delineating Buildings by Grouping Lines with MRFs”, Image Processing, IEEE Transactions on Volume 5, Issue 1, Jan 1996, Page(s):164 - 168
- [4] Rodriguez C.E., Hanwood D., Davis L.S., “An Appearance-Based Approach to Object Recognition in Aerial Images”, Technical Report CS-TR-3380, Computer Vision Laboratory, Center for Automation Research, University of Maryland, Dec, 1994.
- [5] Liow Y., Pavlidis T., “Use of Shadows for Extracting Buildings in Aerial Images”, Computer Vision, Graphics and Image Processing. vol. 49, 1990, pp 242-277.
- [6] Krishnamachari S., Chellappa R., “An Energy Minimization Approach to Building Detection in Aerial Images”, Acoustics, Speech, and Signal Processing, 1994. ICASSP-94., 1994 IEEE International Conference on Volume v, Issue , 19-22 Apr 1994 Page(s):V/13 - V/16 vol.5

- [7] Menet S., Marc P.S., Medioni G., “Active Contour Models: Overview, Implementation and Applications”, Systems Man and Cybernetics, Conference Proceedings., IEEE International Conference on Volume , Issue , 4-7 Nov 1990, Page(s):194 - 199
- [8] Persson M., Sandvall M., Duckett T., “Automatic Building Detection from Aerial Images for Mobile Robot Mapping”, Computational Intelligence in Robotics and Automation, CIRA 2005, Proceedings. 2005 IEEE International Symposium on Volume , Issue , 27-30 June 2005, Page(s): 273 – 278
- [9] Ortner M., Descombes X., Zerubia J., “Building Extraction from Digital Elevation Model”, In Proc. IEEE International Conference on Acoustics, Speech and Signal Processing (ICASSP), Honk Kong, 2003
- [10] Minghong X., Kun F., Yirong W., “Building Recognition and Reconstruction from Aerial Imagery and LIDAR Data”, Radar, 2006. CIE '06. International Conference on. Oct. 2006, pp.1-4.
- [11] Jinghui D., Veronique P., Hanqing L., “Building Extraction in Urban Areas from Satellite Images Using GIS Data as Prior Information”, Geoscience and Remote Sensing Symposium, 2004. IGARSS apos;04. Proceedings. 2004 IEEE International Volume 7, Issue , 20-24 Sept. 2004, Page(s):4762 - 4764
- [12] Levitt S., Aghdasi F., "An Investigation into the Use Of Wavelets And Scaling For the Extraction Of Buildings in Aerial Images", Communications and Signal Processing, 1998. COMSIG '98. Proceedings of the 1998 South African Symposium on , vol., no., 7-8 Sep 1998, pp.133-138,
- [13] Liang T., Weixin X., Jianjun H., “Automatic High-Rise Building Extraction from Aerial Images”, 5th World Congress on Intelligent Control and Automation, June 15-19, 2004 Volume:4, Page(s) 3109-3113

- [14] Pesaresi M., Benediktsson J.A., "Classification of Urban High-Resolution Satellite Imagery Using Morphological and Neural Approaches", Geoscience and Remote Sensing Symposium, 2000. Proceedings. IGARSS 2000, IEEE 2000 International Volume 7, Issue, 2000, Page(s): 3066-3068
- [15] Wei L., Prinnet V., "Building Detection from High-resolution Satellite Image Using Probability Model" IGARSS05, Seoul, Korea, July 2005
- [16] Lin C.A., Nevatia R., "Building Detection and Description from a Single Intensity Image," Computer Vision and Image Understanding, vol. 72, no. 2, Nov. 1998, pp. 101-121
- [17] Lin C., Nevatia R., "Buildings Detection and Description from Monocular Aerial Images", Proc. ARPA Image Understanding Workshop, Feb.1996, pp. 461-468
- [18] Lin C., Huertas A., Nevatia R., "Detection of Buildings Using Perceptual Grouping and Shadows" IEEE Proceedings of Computer Vision and Pattern Recognition 1994, pp62-69.
- [19] Noronha S., Nevatia R., "Detection and Modeling of Buildings from Multiple Aerial Images" IEEE Transactions on pattern analysis and machine intelligence, vol.23 no.5, may2001
- [20] Koç D., Türker M., "Automatic Building Detection from High Resolution Satellite Images", Proceedings on 2nd International Conference on Recent Advances in Space Technologies, 2005. RAST2005, pages 617-622.
- [21] Vinson S., Laurent D.C., Perlant F., "Extraction Of Rectangular Buildings In Aerial Images", In Proc.Scandinavian Conference on Image Analysis (SCIA'01) June 2001,Bergen,Norway

- [22] Lari Z., Ebadi H., “Automated Building Extraction from High-Resolution Satellite Imagery using Spectral and Structural Information Based on Artificial Neural Networks”, Conference on Information Extraction from SAR and Optical Data, with Emphasis on Developing Countries, 2007
- [23] Bowyer K., Kranenburg C., Dougherty S., “Edge Detector Evaluation Using Empirical ROC Curves”, Computer Vision and Pattern Recognition, 1999. IEEE Computer Society Conference on, vol.1, no., 1999, pp.-359
- [24] <http://www.pages.drexel.edu/~weg22/edge.html> last accessed date: 20.11.2008
- [25] Duda R.O., Hart P.E., “Use of the Hough Transformation to Detect Lines and Curves in Pictures”, Comm. ACM, Vol. 15, Jan. 1972, pp. 11–15
- [26] Hough P.V., “Machine Analysis of Bubble Chamber Pictures”, Proc. Int. Conf. High Energy Accelerators and Instrumentation, 1959
- [27] <http://homepages.inf.ed.ac.uk/rbf/HIPR2/hough.htm#1> last accessed date: 20.11.2008
- [28] Ballard D., Brown C., Computer Vision, Prentice-Hall, 1982, Chap. 4.
- [29] Chan C.K., Sandler M.B., “A Complete Shape Recognition System Using the Hough Transform and Neural Network”, Pattern Recognition, 1992. Vol.II. Conference B: Pattern Recognition Methodology and Systems, Proc.
- [30] Chatzis V., Pitas I., “Introducing the Select and Split Fuzzy Cell Hough Transform”, Pattern Recognition, 1996., Proceedings of the 13th International Conference on , vol.2, no., 25-29 Aug 1996, pp.552-556

- [31] Ioannou D., Dugan E.T., "Parallelogram Detection in a Digital Image with the Use of the Hough Transform", Pattern Recognition, 1996, Proceedings of the 13th International Conference on , vol.2, no., 25-29 Aug 1996, pp.532-536
- [32] Tuytelaars T., Gool L.V., Proesmans M., Moons T., "The Cascaded Hough Transform as an Aid in Aerial Image Interpretation", Computer Vision, 1998. Sixth International Conference on, vol., no., 4-7 Jan 1998, pp.67-72
- [33] Hu Z.Y., Tang M., Tsui H.T., "Direct Triangle Extraction by a Randomized Hough Technique", 14th International Conference on Pattern Recognition (ICPR'98)-Volume 1, 1998, pp.717
- [34] Lee H.M., Kittler J., Wong K.C., "Generalised Hough Transform in Object Recognition", Pattern Recognition, 1992. Vol.III. Conference C: Image, Speech and Signal Analysis, 1992
- [35] Ballard D.H., "Generalizing the Hough Transform to Detect Arbitrary Shapes", In Readings in Computer Vision: Issues, Problems, Principles, and Paradigms, M. A. Fischler and O. Firschein, Eds. Morgan Kaufmann Readings Series. Morgan Kaufmann Publishers, San Francisco, CA, 1987, pp.714-725
- [36] Barrett W.A., Petersen K.D., "Houghing the Hough: Peak Collection for Detection of Corners, Junctions and Line Intersections", Computer Vision and Pattern Recognition, 2001, Proceedings of the 2001 IEEE Computer Society Conference on , vol.2, no., 2001, pp. II-302-II-309 vol.2
- [37] Yla A.J., Kiryati N., "Adaptive Termination of Voting in the Probabilistic Circular Hough Transform", Pattern Analysis and Machine Intelligence, IEEE Transactions on, vol.16, no.9, Sep 1994, pp.911-915

- [38] Bennett N., Burrige R., Saito N., "A Method to Detect and Characterize Ellipses Using the Hough Transform", Pattern Analysis and Machine Intelligence, IEEE Transactions on , vol.21, no.7, Jul 1999, pp.652-657
- [39] Tsuji S., Matsumoto F., "Detection of Ellipses by a Modified Hough Transformation", Computers, IEEE Transactions on, vol.C-27, no.8, Aug. 1978, pp.777-781
- [40] Aijun C., Jinzong L., Bing Z., "Circular Object Recognition Based on Shape Parameters", Journal of Systems Engineering and Electronics Volume 18, Issue 2, 2007, Pages 199-204.
- [41] Jung C.R., Schramm R., "Rectangle Detection Based on A Windowed Hough Transform", Computer Graphics and Image Processing, 2004, Proceedings 17th Brazilian Symposium on, vol., no., 17-20 Oct. 2004, pp. 113-120
- [42] Yao J., Zhang Z., "Hierarchical Shadow Detection for Color Aerial Images", Computer Vision Image Understanding 102, 1 (Apr. 2006), 60-69.
- [43] Tsai V.J.D., "A Comparative Study on Shadow Compensation of Color Aerial Images in Invariant Color Models", Geoscience and Remote Sensing, IEEE Transactions on, vol.44, no.6, June 2006, pp. 1661-1671
- [44] Jianjun H., Weixin X., Liang T., "Detection of and Compensation for Shadows in Colored Urban Aerial Images", Intelligent Control and Automation, 2004. WCICA 2004. Fifth World Congress on, vol.4, no., 15-19 June 2004, pp. 3098-3100 Vol.4
- [45] Watanabe S., Miyajima K., Mukawa N., "Detecting Changes of Buildings from Aerial Images Using Shadow and Shading Model", Pattern Recognition, 1998.

Proceedings Fourteenth International Conference on, vol.2, no., 16-20 Aug 1998, pp.1408-1412 vol.2

[46] Barnard K., Finlayson G., “Shadow Identification Using Color Ratios”, Proceedings of the IS&T/SID Eighth Color Imaging Conference: Color Science, Systems and Applications, 2000, pp. 97-101

[47] Wu T.P., Tang C.K., “A Bayesian Approach for Shadow Extraction from a Single Image” Computer Vision, 2005. ICCV 2005 Tenth IEEE International Conference on , vol.1, no., 17-21 Oct. 2005, pp. 480-487 Vol. 1

[48] Scanlan J.M., Chabries D.M., Christiansen R.W., “A Shadow Detection and Removal Algorithm for 2D Images”, in Proc. of Int. Conf. on Acoustics, Speech, and Signal Processing (1990) pp. 2057-2060.

[49] Susuki A., Shio A., Arai H., Ohtsuka S., “Dynamic Shadow Compensation of Aerial Images Based on Color and Spatial Analysis”, in Proc. 15th Int. Conf. Pattern Recognition, Barcelona, Catalonia, Spain, Sep. 3–7, 2000, pp. 317–320

[50] Comaniciu D., Meer P., “Mean Shift : A Robust Approach Toward Feature Space Analysis”, IEEE Transactions on pattern analysis and machine intelligence vol. 24, no. 5 May 2002

[51] <http://mathworld.wolfram.com/Line-LineIntersection.html> last accessed date: 20.11.2008

[52] Otsu N., “A Threshold Selection Method from Gray-Level Histograms”, Systems, Man and Cybernetics, IEEE Transactions on Volume 9, Issue 1, Jan. 1979 Page(s):62 – 66